

Aus dem Max-Planck-Institut für Psychiatrie

Geschäftsführende Direktorin: Prof. Dr. Dr. Elisabeth Binder

**Anatomy, structure and function: Understanding extremes in fear  
and anxiety by *in vivo* imaging techniques**

Dissertation

zum Erwerb des Doktorgrades der Medizin

an der Medizinischen Fakultät der

Ludwig-Maximilians-Universität zu München

vorgelegt von

Marie Karolin Franziska Bartmann

aus

Aschaffenburg

2022

Mit Genehmigung der Medizinischen Fakultät  
der Universität München

Berichterstatter: Prof. Dr. Angelika Erhardt

Mitberichterstatter: Prof. Dr. Peter Zwanzger

PD Dr. Thomas Zetzsche

PD Dr. Daniela Eser-Valeri

Mitbetreuung durch den

promovierten Mitarbeiter: PD Dr. Carsten Wotjak

Dekan: Prof. Dr. med. Thomas Gudermann

Tag der mündlichen Prüfung: 24.03.2022

## Abstract (German)

Angsterkrankungen mit ihren unterschiedlichen Formen wie beispielsweise der generalisierten Angststörung nehmen unter den psychischen Erkrankungen des Menschen den größten Anteil ein. Trotz vieler Bemühungen konnten die zugrundeliegenden Pathomechanismen noch nicht abschließend dargelegt werden. Diese Dissertation hat deshalb zum Ziel, anhand eines Tiermodells der generalisierten Angststörung morphologische Unterschiede von Gehirnregionen zu erfassen um diese anschließend mit gezeigten Verhaltensweisen und molekularen Gegebenheiten zu korrelieren.

Mithilfe von *in vivo* MRT-Untersuchungen und voxel-based morphometry (VBM) von Mäusen mit hochängstlichem (HAB) und normalängstlichem Verhalten (NAB) konnten Gehirnregionen identifiziert werden, die sich hinsichtlich ihres Volumens an grauer Substanz (GMV) unterscheiden. Hierbei konnte ich zeigen, dass das GMV in den Gehirnregionen des Striatums und des Hippocampus in HAB Mäusen reduziert ist.

Die Auswahl der nachfolgend durchgeführten Verhaltenstests wurde entsprechend den Regionen, in denen GMV Unterschiede zwischen den beiden Linien bestehen, getroffen. Die Ausführung des Detour-Water Maze Tests und des Rotarodtests blieb unbeeinträchtigt, wohingegen HAB Mäuse im Probe Trial (PT) des Morris Water Maze (MWM) eine geringere Präzision aufwiesen, was mit den GMV Unterschieden des Hippocampus in Einklang zu bringen ist.

Die synaptischen Marker, welche mithilfe von Western-Blots untersucht wurden, ergaben abweichende Proteinlevel (z.B. von Synapsin, SynGap und GAP-43 im Striatum der HAB Mäuse und von PSD-95 und GAP-43 im Hippocampus der HAB Mäuse) zwischen HAB und NAB Mäusen, wobei im Striatum und Hippocampus jeweils andere Proteine Unterschiede aufzeigten. Mit der daraufhin vollzogenen quantitativen Spine-Analyse im Striatum, konnte ich außerdem die erhöhte striatale Spine Anzahl in HAB gegenüber NAB Mäusen bestätigen.

## Abstract

Anxiety disorders in their different forms show a high prevalence in human population. Therefore, their progressive exploration is of considerable importance. Despite all efforts, the underlying pathomechanisms have not been finally clarified. This thesis intends to point out morphological differences of brain regions, using an animal model of generalized anxiety disorder to correlate them with the observed behaviors and molecular conditions.

Using *in vivo* MRI and voxel-based morphometry (VBM) comparing high anxiety (HAB) and normal anxiety behavior (NAB) mice, I identified brain regions that differ in its grey matter volume (GMV). In doing so, I could demonstrate a reduced GMV of the striatum and the hippocampus of HAB mice.

The applied behavioral tests were selected according to the regions differing between the two strains. The performance in the detour water maze test and the rotarod test was unaffected, whereas HAB mice exhibited lower precision during the probe trial (PT) of the Morris Water Maze, which can be brought in line with the hippocampal GMV differences.

Synaptic markers were studied using western blot procedures. I observed diverging protein levels (e.g. Synapsin, SynGap and GAP-43 in the striatum of HAB mice and PSD-95 und GAP-43 in the hippocampus of HAB mice) between HAB and NAB mice. The respective proteins in the striatum were different from those in the hippocampus. After analyzing spines' quantity within the striatum, I could confirm enhanced striatal spine density in HAB compared to NAB mice.

# Content

<b>ABSTRACT (GERMAN)</b> .....	<b>1</b>
<b>ABSTRACT</b> .....	<b>2</b>
<b>CONTENT</b> .....	<b>3</b>
<b>ABBREVIATIONS</b> .....	<b>5</b>
<b>1 INTRODUCTION</b> .....	<b>7</b>
1.1 ANXIETY DISORDERS .....	7
1.2 GREY MATTER VOLUME AND THE UNDERLYING MECHANISMS .....	9
1.3 ANIMAL MODELS.....	13
1.4 AIMS OF THE STUDY .....	15
1.4.1 <i>Macroscopic differences in brain volume between HAB and NAB mice</i> .....	15
1.4.2 <i>Identifying differences in behavioral correlates between HAB and NAB mice</i> .....	15
1.4.3 <i>Identifying differences in cellular and molecular correlates between HAB and NAB mice</i> .....	15
<b>2 MATERIAL AND METHODS</b> .....	<b>16</b>
2.1 ANIMALS.....	16
2.2 <i>IN VIVO</i> MAGNETIC RESONANCE IMAGING .....	16
2.3 BEHAVIORAL TESTING .....	17
2.3.1 <i>Rotarod Behavioral Task</i> .....	17
2.3.2 <i>Water Maze Navigation Tasks</i> .....	18
2.4 WESTERN BLOT PROCEDURE .....	20
2.5 HISTOLOGICAL ANALYSIS .....	24
2.5.1 <i>Golgi Staining</i> .....	24
2.5.2 <i>Neuronal Reconstruction</i> .....	24
2.6 STATISTICAL ANALYSIS.....	26
<b>3 RESULTS</b> .....	<b>28</b>
3.1 <i>IN VIVO</i> MRI: REDUCED GREY MATTER VOLUME IN THE STRIATUM AND CA3 REGION IN HAB COMPARED TO NAB MICE .....	28
3.2 BEHAVIORAL CORRELATES.....	30
3.2.1 <i>HAB and NAB mice perform similar in the rotarod test</i> .....	30
3.2.2 <i>HAB and NAB mice learned during the Detour Water Maze paradigm</i> .....	32
3.2.3 <i>HAB and NAB mice performed differently in the Morris Water Maze</i> .....	33

# Content

---

3.3	LEVELS OF SYNAPTIC DENSITY PROTEINS – MOLECULAR CORRELATES .....	35
3.3.1	<i>Striatum</i> .....	35
3.3.2	<i>Hippocampus</i> .....	37
3.4	HAB MICE SHOW AN INCREASED SPINE DENSITY IN THE STRIATUM .....	39
<b>4</b>	<b>DISCUSSION .....</b>	<b>42</b>
4.1	ANXIETY AND BRAIN VOLUME .....	43
4.2	BEHAVIORAL CORRELATES FOR THE REGIONS OF ALTERED GREY MATTER VOLUME .....	46
4.2.1	<i>Synaptic plasticity within the CA3-region of the dorsal hippocampus might contribute to the enhanced spatial precision of NAB mice .....</i>	<i>46</i>
4.2.2	<i>The rotarod test may not be the proper task to represent the volume differences between HAB and NAB mice .....</i>	<i>49</i>
4.3	POTENTIAL CELLULAR AND MOLECULAR CORRELATES OF GMV CHANGES IN HAB MICE .....	50
4.3.1	<i>An interpretation of the hippocampal western blot results would require valid quantitative spine analysis for the hippocampus.....</i>	<i>50</i>
4.3.2	<i>Increased spine density, reduced striatal GMV and spine markers in HAB mice – a compensation? .....</i>	<i>52</i>
4.4	HUMAN EQUIVALENCES.....	53
<b>5</b>	<b>SUMMARY AND OUTLOOK.....</b>	<b>56</b>
	<b>BIBLIOGRAPHY .....</b>	<b>60</b>
	<b>ACKNOWLEDGMENT .....</b>	<b>74</b>
	<b>AFFIDIVAT .....</b>	<b>75</b>
	<b>CURRICULUM VITAE .....</b>	<b>FEHLER! TEXTMARKE NICHT DEFINIERT.</b>

## Abbreviations

AMPAR	$\alpha$ -amino-3-hydroxy-5-methyl-4-isoxazolepropionic acid receptor
APS	ammonium persulfate
BAC	bed nucleus of the anterior commissure
BCA-assay	bicinchoninic acid assay
CA	cornu ammonis
Ca <sup>2+</sup>	Calcium
CaMKII	Ca <sup>2+</sup> /calmodulin-dependent protein kinase II
CBT	cognitive behavioral therapy
CP	caudate putamen
CSF	cerebrospinal fluid
DG	dentate gyrus
DL	dorsolateral
DM	dorsomedial
dmPAG	dorsomedial part of the periaqueductal grey
DSM	diagnostic and statistical manual of mental disorders
EPM	elevated plus maze
EU	European Union
FWE	family-wise error
GAD	generalized anxiety disorder
GAP-43	growth-associated protein-43
GM	grey matter
GMV	grey matter volume
GTP	guanosine-5'-triphosphate
HAB	high anxiety behavior
HPC	Hippocampus
IPN	interpeduncular nucleus
ITI	inter-trial interval
JNK	c-Jun N-terminal kinases
LAB	low anxiety behavior
LS	lateral septum
LTD	long-term depression
LTP	long-term potentiation

## Abbreviations

---

MAP	mitogen-activated protein
MDD	major depressive disorder
MEMRI	manganese enhanced magnetic resonance imaging
MHb	medial habenula
Mn <sup>2+</sup>	manganese
MRI	magnetic resonance imaging
MSN	medium spiny neuron
MWM	Morris water maze
NAB	normal anxiety behavior
NMDA	N-Methyl-d-aspartate
ORBm	medial part of the orbital area
PDZ	post synaptic density protein, drosophila disc large tumor suppressor, zonula occludens-1 protein
PIR	piriform cortex
PKC	protein kinase C
pp	perforant path
PSD	post-synaptic density
PT	probe trial
QTL	quantitative trait locus
Ras	rat sarcoma
SDS	sodium dodecyl sulfate-polyacrylamide
SEM	standard error of the mean
SF	septofimbrial nucleus
SNP	single nucleotide polymorphisms
SNRI	serotonin noradrenaline reuptake inhibitor
SSp-bfd	somatosensory cortex/barrel field
SSRI	serotonin reuptake inhibitor
SynGAP	synaptic GTPase-activating protein
TBS	tris-buffered saline
TBS-T	tris-buffered saline-tween
TQ	target quadrant
TS	triangular septum
VBM	voxel-based morphometry
VSDI	voltage-sensitive dye imaging
WM	white matter

# 1 Introduction

## 1.1 Anxiety Disorders

Over one third of the EU population (164.7 million people) suffer from mental disorders during any given 12-month period. Among mental disorders anxiety disorders represent the largest proportion with a 12-month prevalence of 14 % and approximately 69.1 millions of people affected (Wittchen et al., 2011). In addition, anxiety disorders are associated with high costs to society, both as direct healthcare costs and considerable indirect costs through reduced working capacity, sick days or premature retirement (Rice and Miller, 1998; Andlin-Sobocki and Wittchen, 2005). Anxiety disorders including separation anxiety disorders, selective mutism, specific phobias, social phobia, panic disorders, agoraphobia, generalized anxiety disorders and substance-induced anxiety disorders are among the most persistent mental disorders with spontaneous remission rates lower than 23 % (Wittchen et al., 2000; Bittner et al., 2004; American Psychiatric Association, 2013; Craske et al., 2017).

This indicates the need to diagnose anxiety disorders earliest possible in the course of the disorder, as well as the need for improved treatment options at different stages of the disease. Sensitive biomarkers hold the potential to predict, detect or confirm a diagnosis at any given stage (Biomarkers Definitions Working Group, 2001), like they are frequently used in a variety of somatic disorders. For disorders of the brain, however, the search is ongoing since little, for anxiety disorders no clinically relevant markers exist (Filiou et al., 2011; Craske et al., 2017).

In line with improving the quality of medical care, many attempts were taken to identify neuroanatomical, functional or metabolic alterations associated with specific anxiety disorders. Biomarkers identifying the patient's sensitivity for a specific treatment could enhance the therapy success and could limit the current approach of several pharmacological lines of therapy. Additional therapies include a variety of psychotherapeutic approaches such as cognitive behavioral therapy (CBT) as the most widely-used, evidence-based first-line treatment for anxiety disorders (Bandelow et al., 2014; Bandelow et al., 2015). CBT, as a short-term goal-orientated

intervention aims at the reduction of maladaptive behavior in favor of individual coping mechanisms by using strategies like psychoeducation, cognitive restructuring and systematic exposure to feared stimuli (Craske et al., 2017). An alternative approach, or in combination with CBT to preserve relief of symptoms is the application of pharmaceuticals. Antidepressants like selective serotonin reuptake inhibitors (SSRI) or serotonin noradrenaline reuptake inhibitors (SNRI) are considered the first-line pharmacological treatment for most anxiety disorders (except for specific phobia) (Bandelow et al., 2008; Bandelow et al., 2014). In addition, other pharmacological classes such as benzodiazepines (e.g. diazepam, alprazolam), anti-epileptic drugs (e.g. gabapentin, pregabalin) or atypical antipsychotics (e.g. risperidone, quetiapine) represent alternative options to treat anxiety disorders (Craske et al., 2017). Adult patients, in particular, benefit more by combining pharmacological with psychological treatments than using pharmacotherapy alone (Cuijpers et al., 2009). However, only few patients with mental disorders receive adequate treatment, due, among others, to lacking treatment options (Ormel et al., 2008; Wittchen et al., 2011). Moreover, the threshold until patients with mental disorders consult a professional is high, and only 26 % of them do so at all, whereby too often too much time passes between onset and first treatment. Reasons may include the occurrence of unspecified somatic symptoms, exclusively, the following way of the inaccurately report to the professional as well as the fear of stigmatization. As a consequence, diagnosis is aggravated, not only due to high comorbidity (60–90 %; (Wittchen et al., 2011; First et al., 2014), and the recovery might be delayed (Craske et al., 2017).

Taken all this into account, anxiety disorders lead to a high individual and social economic burden, indicating the importance to identify the underlying neuropathophysiological mechanisms to improve treatment options and, with this, let patients and society benefit.

## 1.2 Grey matter volume and the underlying mechanisms

As an potential attempt to explain dysfunctions underlying certain brain disorders, volumetric changes in brain volumes are frequently researched and reported (Hilbert et al., 2014). Investigating its underlying signature, however, may be difficult due to the complexity of involved structures. The composition of human and rats' grey matter is described (Figure 1), changes may explain differences in the substances' volume.

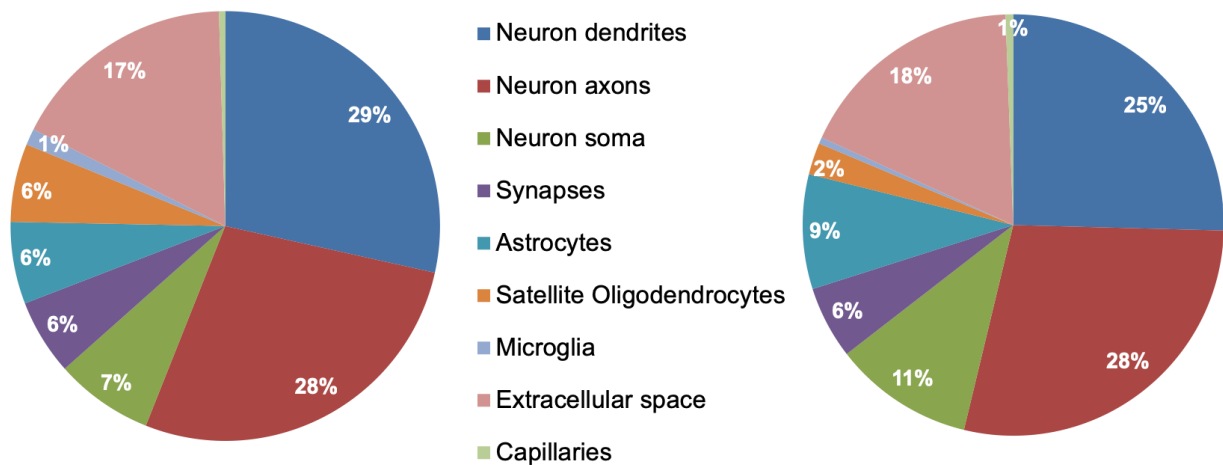


**Figure 1: Composition of grey matter in the brain of humans (left) and rodents (right)** (adapted from Bennett, 2011; Kassem et al., 2013).

Neuronal dendrites (25 – 29 %; rats – humans) and neuronal axons (28 %) have been identified as major representatives of the grey matter substance (Bennett, 2011; Kassem et al., 2013). The extracellular space and astrocytes may have a considerable impact as well, however, the neuronal impact, including soma, is at about 60 %. Studying neurons requires their visualization in slices, for what the Golgi-method is an indispensable technique.

Camillo Golgi (1843–1926) invented this metallic impregnation which is based on fixation of nerve tissue in dichromate in 1873. The consecutive staining is achieved by immersing the nerve tissue in silver nitrate, whereby cells get impregnated by precipitation of silver chromate. The fact that only a small number of neurons are stained in a random manner, allows further investigations of individual cells. The

underlying mechanism of the staining, however, remains still unknown (Kassem et al., 2013). The introduction of Golgi-impregnation paved the way for Santiago Ramón y Cajal (1852–1934) as an advocate of the neuron doctrine. This idea of neurons as independent contiguous units built the cornerstones of our present understanding of neuroscience (Lopez-Munoz et al., 2006; Mazzarello, 2018). It was also Cajal who described dendritic spines as a further possible explanation for volume differences in avian cerebellum in 1888. As tiny protrusions of neuronal dendrites, he assumed that spines contribute to synaptic transmission by connecting axonal boutons with dendritic protrusions and enlarging the dendrites' surface area (DeFelipe, 2015; Gipson and Olive, 2017). Indeed, consecutive studies supported this hypothesis using advanced techniques as high resolution imaging (electron and fluorescence microscopy), molecular techniques and electrophysiology (Gray, 1959; Fairen et al., 1977; Lee et al., 2012; DeFelipe, 2015). Today's knowledge improved and it is known that a spine consists of a neck and the corresponding head that mostly comprises a single synapse (Figure 2). 10 % of the spines' surface is occupied by the electron-dense postsynaptic density (PSD), which is located at the postsynapse exactly opposite the presynaptic active zone and densely covered with receptors and proteins (Hering and Sheng, 2001; Kim and Sheng, 2004).

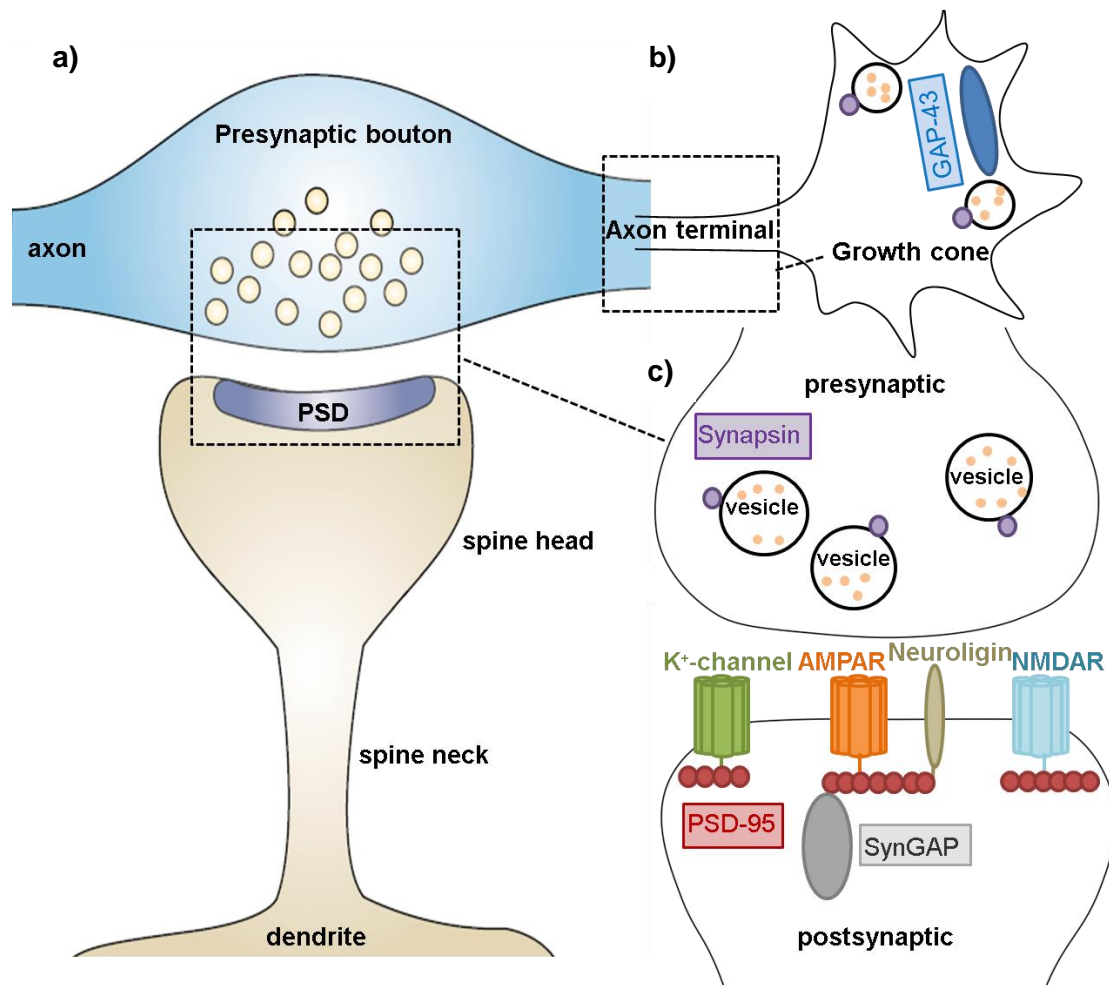


**Figure 2: Schematic illustration of:** (a) a dendritic spine forming the postsynaptic compartment of a synapse (left) and its (b-c) synaptic markers: GAP-43 (b), Synapsin, PSD-95 and SynGAP (c) (adapted from Hering and Sheng, 2001).

Dendritic spines are a key feature of synaptic transmission. Spines, providing plasticity in developmental processes and “learning”, also known as long-term potentiation (LTP), are not static but change their size and shape in an activity dependent manner (Engert and Bonhoeffer, 1999; Hering and Sheng, 2001; Matsuzaki et al., 2004; Murakoshi and Yasuda, 2012; Meyer et al., 2014). The same holds true for dendrites, which constantly form new connections depending on neuronal activities and therewith the release of specific messengers. The dendrite’s growth cone (Figure 2b) plays a major role in sensing its path and groping its surroundings (Pollerberg et al., 2013).

As the growth cone, spines have an individual molecular signature, whereas different proteins are implicated in structure, functionality, motility or elimination (Gipson and Olive, 2017).

In spines, the major component of the structural PSD scaffold is PSD-95, a PDZ-domain containing protein, highly enriched in excitatory synapses (Hering and Sheng, 2001). By anchoring membrane glutamate receptors (e.g. AMPAR, NMDA) and linking them to intracellular cytoskeletal components, PSD-95 is involved in the molecular coordination and facilitation of synaptic transmission (Hering and Sheng, 2001; Kim and Sheng, 2004; Beique et al., 2006). Moreover, it has been shown that PSD-95 contributes to plasticity, strengthening and stabilization of synapses through its recruitment of AMPA receptors to the PSD (Ehrlich et al., 2007; Chen et al., 2011; Meyer et al., 2014).

Interacting with the PDZ-domains of PSD-95, the synaptic GTPase-activating protein (SynGap) is abundantly expressed at the PSD of excitatory synapses, too (Kim et al., 1998). The hydrolase SynGap becomes inactivated by CaMKII (Ca<sup>2+</sup>/calmodulin-dependent protein kinase II) through its phosphorylation and thus, negatively regulating Ras through the MAP (mitogen-activated protein) kinase signaling pathway (Chen et al., 1998). During LTP, SynGap is involved in trafficking AMPA receptors to synapses in an NMDAR and CaMKII-dependent manner (Krapivinsky et al., 2004; Yang et al., 2013; Araki et al., 2015).

The molecular signature of presynaptic growth cones include the membranous growth-associated protein-43 (GAP-43; Figure 2b; Goslin et al., 1988) which promotes axonal growth after its phosphorylation by PKC or JNK (Benowitz and Routtenberg, 1997; Holahan, 2017; Kawasaki et al., 2018).

In contrast to the postsynaptic PSD, the phosphoprotein Synapsin I enriches at presynaptic sites of axonal terminals and growth cones (Fletcher et al., 1991). With its different isoforms (Synapsin Ia and Ib), the protein is implicated in the release of synaptic vesicles. Under resting state, Synapsin stays dephosphorylated and is bound to the cytoplasmic surface of vesicles (Greengard et al., 1993). Influx of Ca<sup>2+</sup>, however, triggers processes as the activation of CaMKII, which then phosphorylates Synapsin (De Camilli et al., 1990). Subsequently, Synapsin dissociates from the release pool, vesicles move to the active zone and neurotransmitters are released. Moreover, Synapsin is, like GAP-43, involved in neuronal plasticity and neuronal growth (Cesca et al., 2010; Nikolaev and Heggelund, 2015).

### 1.3 Animal Models

Animal models are shown to gain a high translational value. A major focus comes to rodents, through their advantages in breeding and genetics as well as their homologies to humans in neuronal structures implicated in fear and anxiety (Calhoun and Tye, 2015).

Although DSM does not distinguish between fear and anxiety in terms of diagnosing and treatment of anxiety disorders in humans, it is common to do so in basic and animal research. The distinction between fear and anxiety is based on the imminence of threat and the duration of response (LeDoux and Pine, 2016; Craske et al., 2017). Fear typically occurs in response to imminent, clearly perceived threats. It facilitates an immediate escape from the threat and usually dissipates on removal of the eliciting stimulus. Anxiety responses, in contrast, are characterized by long-acting, more generalized distal threats that do not pose direct endangerment. The state of anxiety is accompanied by subjective experiences like worried thoughts and tension. Anxiety-specific, future-focused responses help to stay prepared by increased awareness and risk assessment (Davis et al., 2010; Gross and Canteras, 2012; Calhoun and Tye, 2015; LeDoux and Pine, 2016), whereas persisting, excessive anxiety is considered pathological and may lead to anxiety disorders (Calhoun and Tye, 2015).

Increasing the translational potential of animal studies, animal models should fulfil three validity criteria (McKinney and Bunney, 1969; Holsboer and Ströhle, 2005): (1) established pharmacological treatments from the human situation should be sufficient in the animal model as well (*predictive validity*; (Cryan and Holmes, 2005). (2) *Face validity* ensures the validity of symptoms and responses that should be comparable in its behavioral and physiological appearance between humans and animal models. However, (3) *etiological validity* as the formation of symptoms, and the (4) underlying neurobiological processes causing the disease (*construct validity*) are not trivial to include in the case of anxiety disorders, since little of the causes and the underlying mechanisms is known (Siegmund and Wotjak, 2006; Calhoun and Tye, 2015).

A classical test situation, together with appropriate readouts and the model organism forms an animal model.

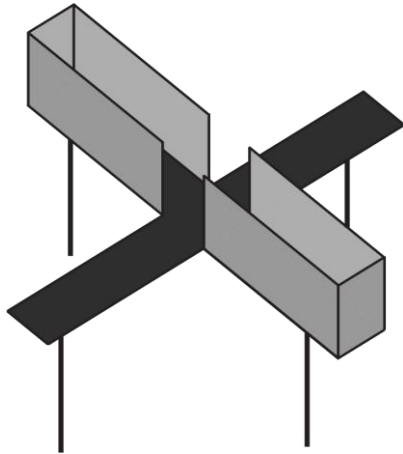


**Figure 3: Elevated Plus Maze.** The EPM consists of two open and two enclosed opposing arms. Mice tend to spend more time on the enclosed arms of the maze are considered to be more anxious and vice versa.

At the beginning of a test procedure, the mouse is placed in the central part of the maze facing a closed arm. The degree of avoidance of the open arms is interpreted as the respective anxiety behavior. Thus, more anxious mice tend to avoid the open arms and less anxious behavior correlates with mice spending more time on the open arms of the maze.

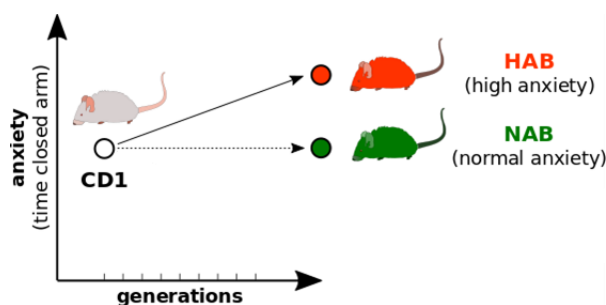


**Figure 4: HAB and NAB mice.** Behavioral read-outs of the EPM were used as a classification, and breeding criterion for high anxiety (HAB) and normal anxiety (NAB) mice (adapted from Krömer et al., 2005).

The elevated plus maze (EPM), for instance, was first validated in 1985 as a paradigm to test unconditioned anxiety (Pellow et al., 1985). The apparatus consists of an elevated plus-shaped maze with two opposing open arms (unprotected) and two facing arms that are enclosed by sidewalls (

Figure 3). Considering rodents' natural aversion to novel, open and unprotected areas (Belzung and Le Pape, 1994), exposure to elevated open arms provokes a stronger approach-avoidance conflict than it would for enclosed arms (Lister, 1987; Belzung and Le Pape, 1994; Calhoun and Tye,

In my thesis, I focused on both mouse lines, mimicking the state of generalized anxiety disorders to investigate underlying characteristics of high versus normal anxiety behavior.

## **1.4 Aims of the Study**

The underlying mechanisms of pathological anxiety remain mostly unknown. Using the model system of high anxiety behavior (HAB) mice with the normal anxiety behavior (NAB) mice as a control condition, I am interested in potential differences in (1) the grey matter volume, its (2) behavioral consequences and its (3) cellular and molecular correlates.

### **1.4.1 Macroscopic differences in brain volume between HAB and NAB mice**

To investigate whether HAB and NAB mice show divergent macroscopic alterations in their brain volumes, I performed volumetric MRI-scans. A voxel-based morphometric (VBM) analysis allowed to compare the entire brain on volumetric changes in grey matter between the groups.

### **1.4.2 Identifying differences in behavioral correlates between HAB and NAB mice**

In a next step, I wanted to investigate if the region-specific differences in grey matter volumes manifest in a behavioral phenotype. Therefore, I performed specific behavioral tasks, phenotyping HAB and NAB mice addressing hippocampus-dependent learning processes (Morris Water Maze; MWM) as well as striatum-dependent motor coordination and learning (rotarod).

### **1.4.3 Identifying differences in cellular and molecular correlates between HAB and NAB mice**

Investigating the underlying mechanisms of in 1.4.1 encountered regions, I performed Western blot procedures with several specific antibodies targeting proteins that are involved in the continuity of spines' function. Potential molecular differences might correlate with the received volume differences and, therewith may explain them.

As a last step, I studied the dendritic morphology of the candidate regions using Golgi-staining of brain slices.

## 2 Material and Methods

### 2.1 Animals

Experiments were carried out on male High Anxiety Behavior (HAB; n=39) and Normal Anxiety Behavior (NAB; n=42) mice at the age of 3 to 9 month. Mice were selectively bred at the animal facility of the Max Planck Institute of Biochemistry (Martinsried, Germany) in accordance to Kroemer and colleagues (2005). Animals were housed at the Max Planck Institute of Psychiatry under standard housing conditions (23°C ± 4°C and 50 % humidity ± 10 %) in groups in individually ventilated cages (IVC; Tecniplast Green Line, Hohenpeißenberg, Germany). Cages are equipped with enrichment tubes (rectangular; Abedd, Vienna, Austria), bedding and *ad libitum* access for food (1314, Altromin Spezialfutter GmbH & Co. KG, Lage, Germany) and water. Experiments took place during the light phase of the animals (lights on: 7 am to 7 pm). All animal studies were in agreement with the government of Upper Bavarian (AZ: ROB-55.2-2532.Vet\_02-17-224) and were conducted in accordance with the recommendations of the Federation for Laboratory Animal Science Associations and according to the European Community Council Directive 2010/63/EEC.

### 2.2 *In vivo* Magnetic Resonance Imaging

HAB and NAB mice underwent single volumetric MRI-scans. Mice were anesthetized using Isoflurane (Isofluran CP<sup>®</sup>, cp-pharma<sup>®</sup>, Burgdorf, Germany). Anesthesia was introduced at a concentration of 2.0 % (air flow around 1.5 l/min) and maintained at 1.5–2.5 % throughout the scanning procedure (aiming at a respiration rate of 90–100 bpm). Animal's eyes were covered with cream (Bepanthen<sup>®</sup> Bayer AG, Leverkusen, Germany) to protect them from drying out. Animals were positioned on a custom-made animal bed in prone position, and stereotactically fixated. Mice were placed onto a heating pad (by water bath, Haake S 5P, Thermo Fisher Scientific,

Waltham, United States) and a respiration pillow. Body temperature was monitored by positioning a rectal probe (maintaining at 37°C).

Paravision (Paravision 6.0.1, Bruker, Ettlingen, Germany) was used to operate the MRT (9.4T Bruker, Ettlingen, Germany) and to perform a volumetric scan. All experiments were performed using a transmit/receive cryogenic coil, in order to optimize signal-to-noise ratio. First of all, the “Localizer” was selected, followed by adjustment of the coil’s impedance (“wobbling”). Then the “localizer”, which serves as an orienting overview of different layers and facilitates the geometrical planning of subsequent sequences, was started. Afterwards the “localizer\_multi\_slice” was conducted, collecting more slices in all three orientations, followed by the acquisition of a “B0-Map” to allow for automated shimming (i.e. homogenizing the magnetic field at the location of the mouse brain), and the “Reference-Power” (to adjust the transmitter power to the superior part of the brain close to the transmitter coil). Following this, a 1h lasting “T1-FLASH” was collected (TE: 6.25 ms; TR: 34.11 ms; averages: 3; repetitions: 1; acquisition matrix: 256x166x218; image size: 256x166x205; resolution: 0.077x0.077x0.077 mm). When the “T1-FLASH” has succeeded, anesthesia was faded out and mice were placed back in their cages. Total time of anesthesia was between 1–1.5 h per mouse. Recovery of the animals was monitored. Images were analyzed as described in 2.6, statistical analysis.

## 2.3 Behavioral Testing

### 2.3.1 Rotarod Behavioral Task

In order to assess motor coordination and motor learning skills, new groups of NAB (n=12) and HAB (n=12) mice were tested at the Rotarod task (ROTA-ROD for mice; Ugo Basile, Gemonio, Italy). The apparatus consisted of five separated partitions (Figure 10a), so that five mice could be tested at once. Mice were placed upon the rotating rod, which is turning forward at a speed of 5 rpm and were expected to start walking in order to stay on the rod. The defined protocol included an acceleration of the rod’s rotation (from 5 to 50 rpm in 5 minutes), starting as soon as all mice were placed. The latency until they touch the bottom plate is recorded automatically for each mouse by a corresponding magnetic sensor at the bottom plate. Fallen mice were placed back to the cage, the rod kept rotating until all mice fall or the end of the

trial was reached. In my protocol, four mice were tested at once (cage wise) at low light conditions (5 lux) three times a day (inter-trial intervals (ITI) of 60 min) on three consecutive days and on day ten. Between the trials, rod and plates were cleaned with water containing detergent. Animals' body weight was measured by weighing prior testing at day 1.

### 2.3.2 Water Maze Navigation Tasks

The same mice which underwent the rotarod test (2.3.1) were tested in two spatial learning protocols: In the *detour paradigm*, mice were tested for their cognitive flexibility, in the *Morris Water Maze* for classical spatial learning capabilities. Tests were performed in a circular water maze built of white synthetic (diameter: 160 cm, walls: 40 cm height) under low light conditions. Around the centrally placed arena, spatial landmarks (from N clockwise: black circle, black square, black plus, black triangle) were placed onto the walls of the room. The experimenter stayed at the north position throughout the entire experiments. Animals were transferred cage-wise to the experimental room (to a bench located right next to the experimenter's position) and stayed there until all animals of the cage were tested. The maze was filled with fresh water at room temperature (21-22°C) at the beginning of the experiment.

For the detour experiment, water was filled up to 10.5 cm, 1 cm above the transparent platform (l: 9.5 cm, w: 8 cm, d: 8 cm). The platform was placed in the center of the maze and was tagged with a black flag (h: 16 cm, w: 6 cm). Facing the wall, mice were started four times a day for three consecutive days in a pseudorandomized order (d1: N, S, W, E; d2: W, E, N, S; d3: S, W, E, N). Mice were trained to reach the platform within one trial (60 s). If a mouse did not find the platform within the trial, it was gently guided to it using a scoop. After reaching the platform, mice were transferred to their home cage by using the scoop. Between the trials, mice got at least 5 min to recover. After the last trial, the mouse's cage was partially placed under a heating lamp for 20 min. On day 4 and 5, the access to the platform from one half of the circumference was impeded by a transparent barrier (Figure 5; l: 35 cm x w: 26 cm, oriented in a 90° angle). The barrier was placed on the side of the starting position. Mice were started in a pseudorandomized order (d4:

E, N, S, W; d5: N, E, W, S) with the barrier moving accordingly. All trials were video recorded using ANY-maze 7 (Behavioral Tracking software; Dublin, Ireland) and analyzed accordingly.

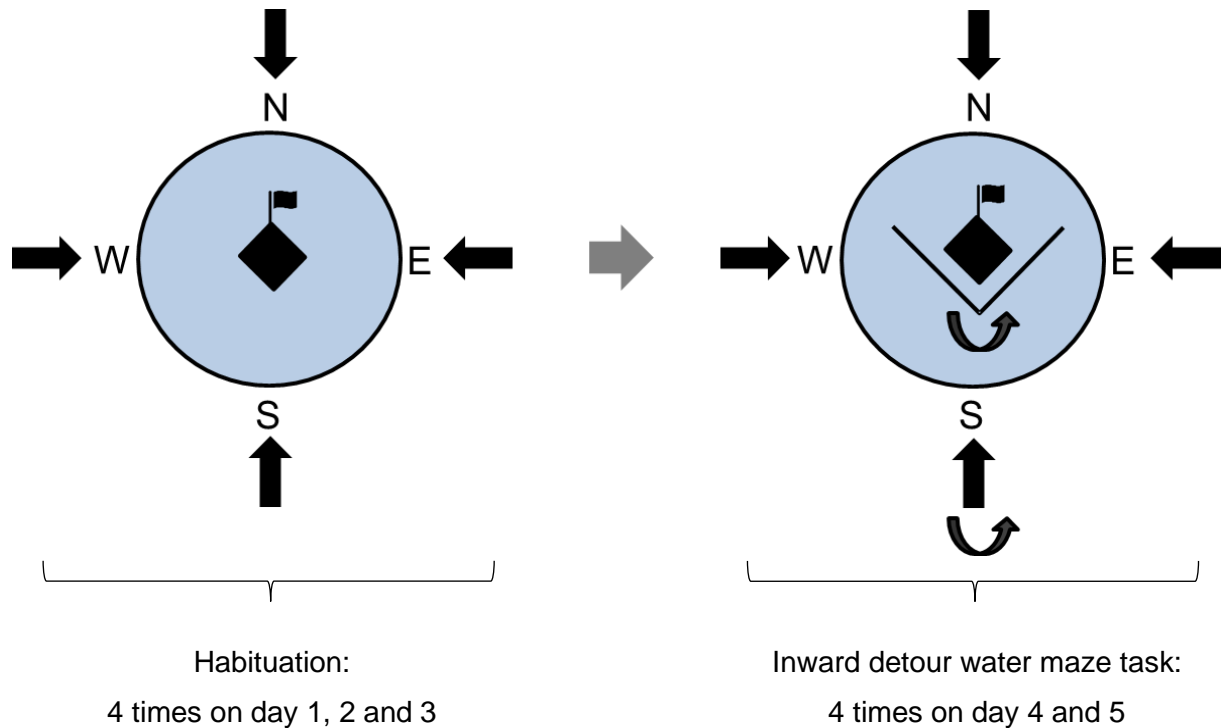


**Figure 5: Detour Water Maze testing protocol.** Starting positions and corresponding position of the barrier (arrows) were changed in a pseudorandomized order.

For the Morris Water Maze (MWM) experiment, water was filled up to 32 cm, 1 cm above a transparent circular platform (h: 31 cm, d: 10 cm). Platform position was maintained in the northwest zone throughout the experiments (day 1-4). Each mouse was given 4 trials a day for 4 consecutive days with an ITI of at least 5 min. Facing the wall, mice were started from a possible starting point that was chosen in a pseudorandomized order (d1: S, W, SE, SW; d2: NE, W, E, S; d3: E, SW, SE, N; d4: W, E, N, SE). Mice were allowed to search for the hidden platform for up to 60 seconds. If a mouse did not manage to locate the platform within the 60 s, it was guided to it and a latency of 61 s was noted. After the mouse reached the platform and stayed for at least 5 s, it was transferred to its home cage by using a scoop. After

the last trial, cages were partially placed under a heating lamp for 20 min. On day 5, the platform was removed, and spatial memory retention was assessed during a probe trial (PT). Mice were started opposite to the previous platform position (d5: SE). Classical parameters like swimming paths, time spent in quadrants [%], distance travelled in quadrants expressed as percentage of the total swimming path length [%], average distance from platform [m] and platform crossings [#] were recorded and further analyzed using ANY-maze 7 (Behavioral Tracking software; Dublin, Ireland).

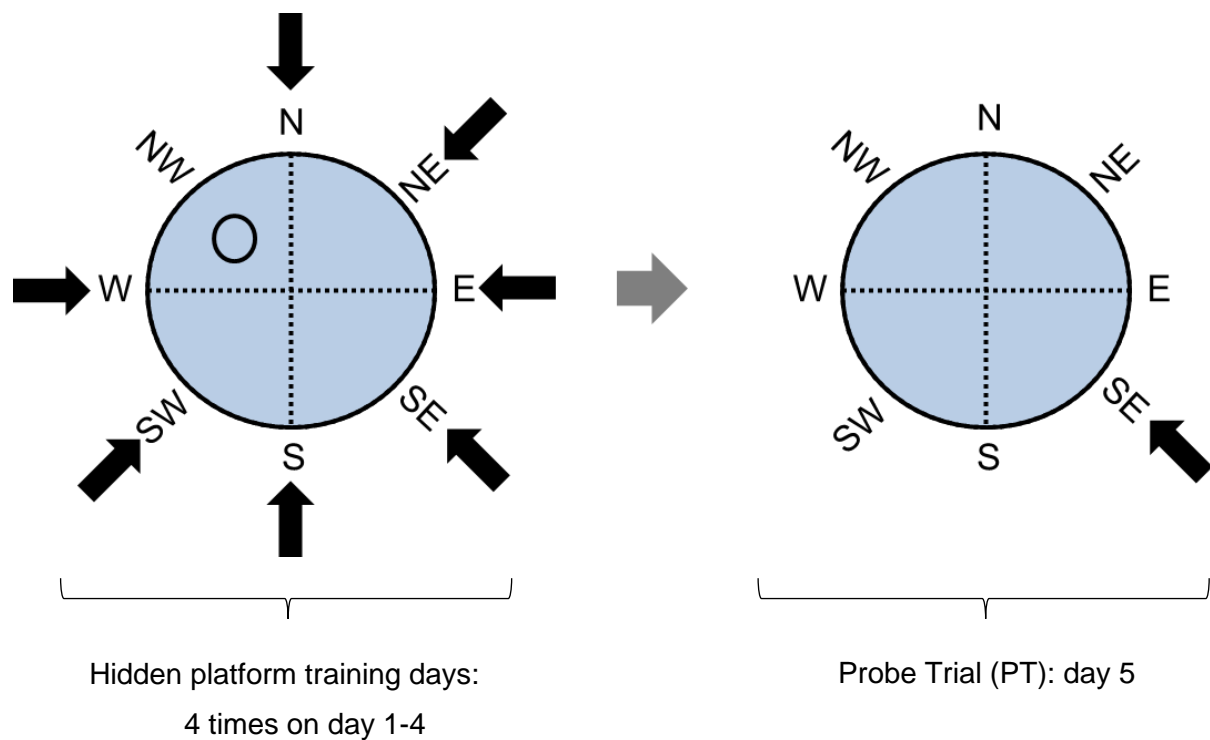


**Figure 6: Experimental setup of the Morris Water Maze (MWM) task.** Starting positions (arrows) were changed in a pseudorandomized order on day 1-4. On day 5 mice were started from the opposite position (SE) of the TQ (NW).

## 2.4 Western Blot Procedure

Biopsies were collected bilaterally from striatum and the dorsal hippocampus (containing CA3-region) using mouse punches (internal diameter of 2 mm; Figure 7)

at -20°C in a cryostat (Microm HM 560, Thermo Scientific, Walldorf, Germany) and region-specific collected in pre-chilled collection tubes (Protein LoBind, Eppendorf AG, Hamburg, Germany). Biopsies were stored at -80°C. To 100 µL of homogenization buffer (50 mM Tris pH 7.5, 150 mM NaCl, 5 mM EDTA) the protease inhibitor mix (Roche; Basel, Switzerland) was freshly added and dissected brain tissue was manually homogenized using a plastic mortar. Afterwards, the same volume of extraction buffer (50 mM Tris pH 7.5, 150 mM NaCl, 1 % NP-40, 1 % Deoxycholate, 2 % SDS, protease inhibitor mix) was added and samples were sonicated at 30 % duty with an output at 3 for 12 strokes. Proteins were denatured by heating them at 95°C for 10 min, followed by a centrifugation with 14.000 g for 5 min at room temperature. Supernatants were processed and transferred to a fresh collection tube, followed by determining the protein concentration using bicinchoninic acid assay (BCA) (according to the manufactures instructions (Pierce™ BCA Protein Assay Kit, Thermo Scientific, Waltham, United States); Albumin standard: 10 µg; 7.5 µg; 5 µg; 3.75 µg; 2.5 µg; 1.25 µg; 0.625 µg; 0.125 µg and 0 µg).

Protein levels were normalized, and samples prepared for gel electrophoresis by diluting them with sample buffer (5 % SDS, 40 % Glycerine, 160 mM Tris pH 6.8, 5 % β-mercaptho, Bromphenol blue, diluted in H<sub>2</sub>O<sub>dest</sub>) to a final concentration of 2 µg/µL. For performing sodium dodecyl sulfate-polyacrylamide gel electrophoresis (SDS-PAGE), 10 percentage gels were prepared (Stacking gel: H<sub>2</sub>O<sub>dest</sub>, 30 % acrylamide mix, 1.0 M Tris pH 6.8, 10 % SDS, 10 % ammonium persulfate (APS), TEMED; Separating gel: H<sub>2</sub>O<sub>dest</sub>, 30 % acrylamide mix (SERVA electrophoresis GmbH, Heidelberg, Germany), 1.5 M Tris pH 8.8, 10 % SDS, 10 % APS, TEMED).

Protein ladder (2 µL; page ruler plus prestained; Thermo Fisher Scientific) and 35 µg (17.5 µL) sample were loaded on the gel. Electrophoresis was performed at 100 V (Power PAC 300, BIO-RAD, Hercules, United States) in running buffer (2.5 mM Tris, 19 mM glycine, 0.05 % SDS in water; freshly diluted in H<sub>2</sub>O<sub>dest</sub> from 10-fold stock) for 120 min at room temperature.

Shortly afterwards, separated proteins were blotted on a nitrocellulose membrane (Protran 0.2 µm, Amersham™, Chalfont St. Giles, England). Wet transfer in transfer buffer (70 % H<sub>2</sub>O<sub>dest</sub>, 20 % CH<sub>3</sub>OH, 10 % transfer buffer, freshly diluted from 10-fold stock (25 mM Tris, 19 mM Glycin, diluted in H<sub>2</sub>O<sub>dest</sub>)) was performed under 400 mA for 60 min on ice. Success of the transfer was verified by a fast ponceau staining (SERVA electrophoresis GmbH, Heidelberg, Germany), dipping the membrane in the

staining solution, followed by three washing steps (5 min each) in TBS-T (Tween-20 Carl Roth GmbH, Karlsruhe, Germany). Membranes were incubated in milk (milk powder (Carl Roth GmbH, Karlsruhe, Germany) diluted in TBS-T) for 30 min at room temperature, followed by incubation in primary antibodies (Table 1; 1:1000 diluted in TBS-T) at 4°C overnight on a shaker. Before membranes were incubated with the corresponding secondary antibody (Table 1; 1:10000 diluted in TBS-T) for 2 h at room temperature on the shaker, they were washed 3 times in TBS-T for 5 min each. Secondary antibodies were detected using chemiluminescence. To this end, membranes were dipped in chemiluminescence substrate (Immobilon Western Chemiluminescence Kit; Merck Millipore, Darmstadt, Germany) according to the manufacturer's instruction, followed by detection using ChemiDoc imaging (ChemiDoc™ MP Imaging System, BIO-RAD, Hercules, United States). Different lengths of exposure were chosen depending on the signal. For detecting chemiluminescence, the default “chemi high sensitivity” protocol, for the protein ladder, “Alexa 488” default protocol was used. Expression levels were normalized to  $\beta$ -actin per mouse and expressed as percentage of the mean NAB levels.

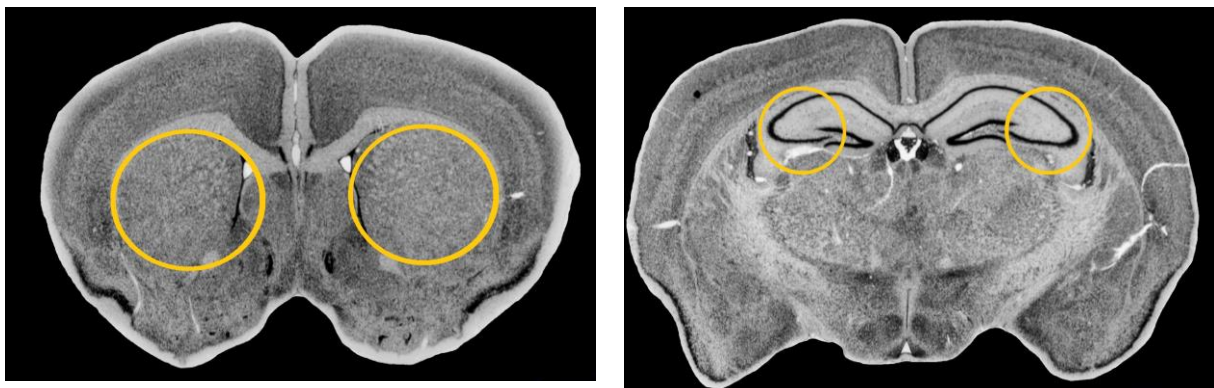


**Figure 7: Striatum (left) and hippocampus (right):** punched regions illustrated as yellow circles.

**Table 1: Antibodies used.** Suppliers: Merck Millipore (Darmstadt, Germany), Cell Signaling (Danvers, United States). Used Antibodies are listed chronologically.

Primary Antibody (protein size, origin and catalog number)		Dilution	Secondary Antibody		Dilution
PSD-95 (95 kDa)  (Mouse monoclonal)	#1598  Merck Millipore	1:1000	anti-Mouse  (HRP-linked)	#7076  Cell Signaling	1:10000
Synapsin-1 (77 kDa)  (Rabbit monoclonal)	#5297  Cell Signaling	1:1000	anti-Rabbit  (HRP-linked)	#8098  Cell Signaling	1:10000
SynGap (140 kDa)  (Rabbit monoclonal)	#5539  Cell Signaling	1:1000			
GAP-43 (43 kDa)  (Rabbit monoclonal)	#8945  Cell Signaling	1:1000			
β-Actin (45 kDa)  (Mouse monoclonal)	#3700  Cell Signaling	1:1000	anti-Mouse  (HRP-linked)	#7076  Cell Signaling	1:10000

## 2.5 Histological Analysis

### 2.5.1 Golgi Staining

Brains of a separate group of HAB (n=6) and NAB (n=6) mice were prepared using the *superGolgi* Kit (Bioenno Tech LLC, Irvine United States) according to manufacturer's recommendations. Mice were deeply anesthetized (Isofluran CP<sup>®</sup>, cp-pharma<sup>®</sup>, Burgdorf, Germany) and decapitated. Brains were removed freshly and placed into light protected 15 mL reaction tubes containing 10 ml Golgi Impregnation Solution comprising potassium dichromate. The solution was replaced after 48 h of incubation at room temperature, followed by additional 14 days. Afterwards, brains were transferred into Post-Impregnation Buffer, which was renewed after 1 day of immersion. After 2 days of post-impregnation, brains were ready for sectioning. Coronal slices with a thickness of 150 µm were sliced using a vibratome (Thermo Fisher Scientific Microm HM 650 V, Walldorf, Germany; frequency: 30 Hz; amplitude: 0.2 mm; speed: 10 mm/s). Until mounting on adhesive (gelatin-coated) microscope slides, slices were collected in dishes containing Collection & Mounting Buffer. Brain sections were allowed to air-dry for about 4-6 h before post-processing according to the manufacturer's protocol. Before embedding with DPX (Mountant for histology, Sigma-Aldrich, St. Louis, United States), brain tissues were dehydrated in 100 % ethanol and defatted in xylene substitute (Xylol (Isomere) Carl Roth GmbH + Co. KG Karlsruhe, Germany).

### 2.5.2 Neuronal Reconstruction

Golgi-stained slides were analyzed and spines of medium spiny neurons (MSN) were quantified. For this, an Axio Imager.M2 microscope (Zeiss, Oberkochen, Germany) with a motorized stage, operated by NeuroLucida software (NeuroLucida<sup>®</sup> version 2017.03.3, MBF Bioscience, Williston, United States), was used.

Dendritic length and number of spines were measured using the NeuroLucida software, subsequent analysis was computed using NeuroLucida Explorer (NeuroLucida<sup>®</sup> Explorer 2017.02.9, MBF Bioscience, Williston, United States). Experimental groups were blinded, and six striatal medium spiny neurons per animal

(three per hemisphere) were selected by an unbiased researcher not involved in subsequent analysis using a 40x lens. MSN included in the analysis were identified by their characteristically stellate shape (spherical dendritic radiation), the presence of at least three primary dendrites and adequate complexity. MSNs that were not isolated from their neighboring neurons and those displayed any obvious truncation or incomplete impregnations were excluded from further processing to prevent incomplete analyzing.

In order to provide a standardized selection of dendritic sections, two concentric circles, anchored at the soma, with a radius of 20  $\mu\text{m}$  and 40  $\mu\text{m}$  were drawn and used as the starting point of the quantification (Figure 8). 4 segments (2 per radius) from one or more dendrites were analyzed from each selected MSN. Cells and segments were digitally labelled using 40x magnifications to ensure a better orientation at a higher magnification. Using a 100x lens, dendritic segments were traced and spines, irrespective of their morphological characteristics, were detected for at least 10  $\mu\text{m}$  from the radius-defined starting point. Secondary information of the analyzed segments as the corresponding branch order (1<sup>st</sup> order = no branch) and the exact scored length of the segment were acquired. The total data set includes 144 segments (4 per neuron) of 36 neurons (6 per animal) from 6 HAB mice and 120 sections (4 per neuron) of 30 neurons (6 per animal) from 5 NAB mice. Due to inferior quality, one NAB brain had to be excluded from analysis; the CA3-region of the hippocampus had to be excluded from analysis due to a too strong Golgi-staining resulting in dendrites not fulfilling the analysis criteria (Figure 16).

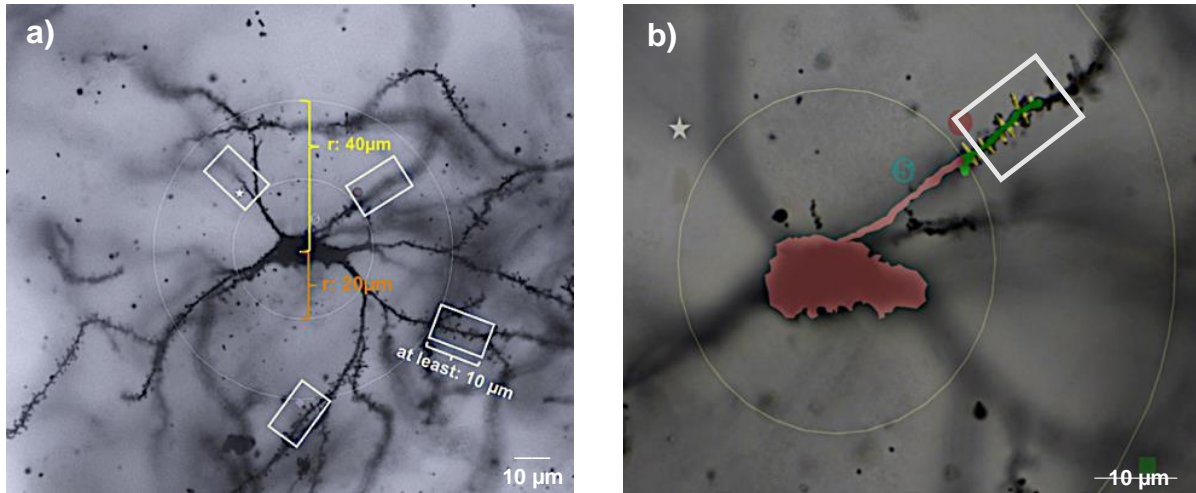


**Figure 8: Morphometric analysis of striatal medial spiny neurons. (a)** Representative striatal medial spiny neuron (MSN) of a NAB mouse (40x). Two concentric circles with a radius ( $r$ ) of 20  $\mu\text{m}$  and 40  $\mu\text{m}$  are illustrated and used as the starting point for the analysis of a  $\geq 10 \mu\text{m}$  segment. **(b)** Representative analysis for one segment at a magnification of 100x.

## 2.6 Statistical Analysis

Data are presented as means with or without individual data. Error bars represent the standard error of the mean (SEM). Results and information about the test and sample sizes are indicated in the text sections and figure legends. Data were analyzed and graphs were generated using GraphPad Prism 8.0 (San Diego, United States). Results were regarded as statistically significant if  $p < 0.05$ .

Preprocessing of the T1w images started with transferring the BRUKER data to Nifti format. In order to exploit the SPM pipeline optimized for human subjects, voxel size of the mouse images was artificially increased 10x. The analysis then followed the recommendations of the VBM tutorial (John Ashburner, March 15, 2010), but using SPM12 and the spmmouse tissue probability maps (again increasing the voxel size by a factor 10). After brain extraction using the Firstsource solutions Ltd brain extraction tool, images were first segmented into grey matter (GM), white matter (WM) and cerebrospinal fluid (CSF) compartments, and DARTEL imported images were created. In a second step, GM and WM were used to create a study template using DARTEL in seven iteration steps. The resulting flow fields were used to normalize the T1w images and the GM images into the group template space,

preserving the amount of the tissue probability. Finally, the images were spatially smoothed with a Gaussian kernel of  $8 \times 8 \times 8 \text{ mm}^3$  (artificial voxel size).

Statistical analysis was performed using a two-sample t-test including data of 10 HAB and 9 NAB mice. Both groups were independent, and an unequal variance was assumed. Global normalization was performed by including the total intracranial volume (GM + WM + CSF) as a factor for proportional scaling. An explicit binary mask based on the mean bet masks was used to exclude outer brain voxel from analysis. A threshold of  $p < 0.001$ , uncorrected, with a minimum cluster extent of 20 voxels was used to identify GM regions showing volumetric differences between the two mouse strains.

### 3 Results

#### 3.1 *In vivo* MRI: Reduced grey matter volume in the Striatum and CA3 region in HAB compared to NAB mice

To characterize the grey matter volume (GMV) of HAB *versus* NAB mice, I performed magnetic resonance imaging (MRI) scans, followed by a voxel-based whole brain analysis. Comparing the morphometric traits of HAB (n=10) and NAB (n=9), a variety of brain structures revealed different between the groups (Figure 9).

Brain structures that showed decreased volumes (Figure 9, depicted in red) in HAB mice compared to NAB mice were: medial part of the orbital area (ORBm), caudate putamen/striatum (CP), piriform cortex (PIR), CA3-region of the dorsal hippocampus (CA3), somatosensory cortex/barrel field (SSp-bfd) and the dorsomedial part of the periaqueductal grey (dmPAG). In contrast, an increased GMV (Figure 9; depicted in blue) was observed in the septofimbrial nucleus/triangular septum (SF/TS) and the hypothalamus, which did not persist after applying the family-wise error (FWE) to correct for multiple testing. Structures decreased in HAB mice, caudate putamen, CA3-region, somatosensory cortex/barrel field and the dorsomedial part of the periaqueductal grey remained significant after correction by the FWE (Figure 9; regions highlighted in bold letters).

Due to the prominent results found in the striatum and the CA3-region of the dorsal hippocampus, I focused on these two regions throughout all further investigations.

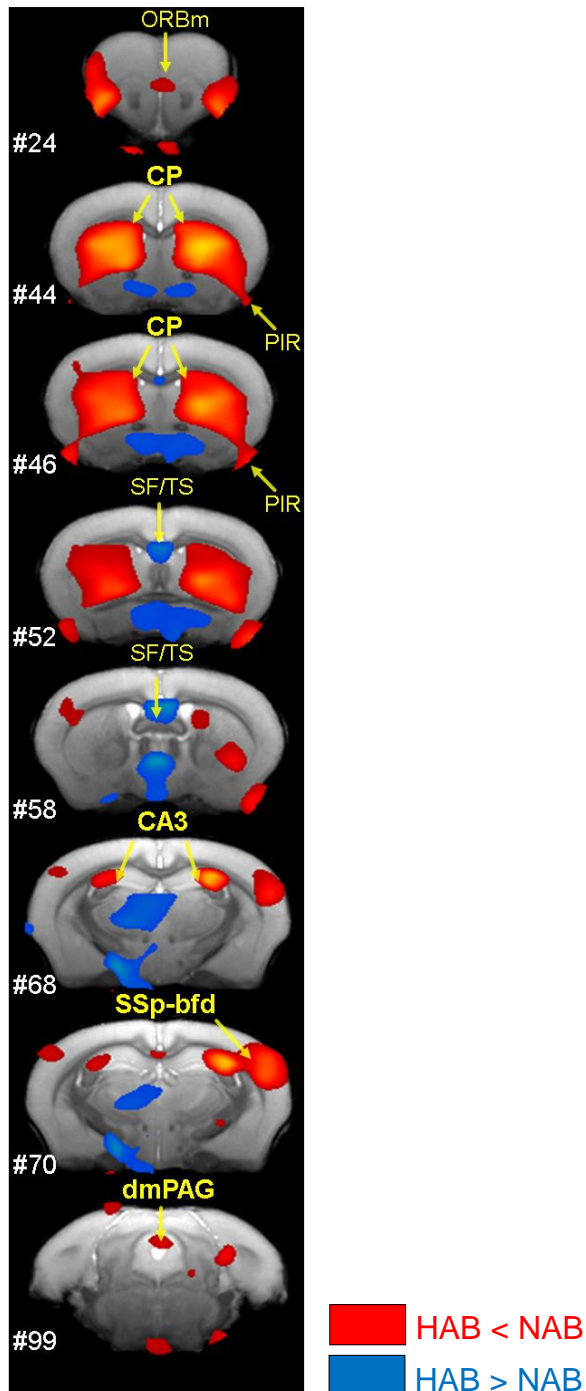


**Figure 9: Differences in grey matter volume (GMV) after voxel-wise morphometry revealed several structures with reduced (red) or increased (blue) GMV in HAB (n=10) vs. NAB (n=9).** Numbers refer to plates from the Allen Mouse Brain Atlas. CA3: CA3-region of the dorsal hippocampus; CP: caudate putamen/striatum; ORBm: orbital area medial part; dmPAG: dorsomedial periaqueductal grey; PIR: piriform cortex/area; SF: septofimbrial nucleus; SSp-bfd: somatosensory cortex/ barrel cortex; TS: triangular septum. Regions highlighted in bold persist to show volume differences after using family-wise error (FWE) correction.

## 3.2 Behavioral Correlates

### 3.2.1 HAB and NAB mice perform similar in the rotarod test

To investigate the animals' motor coordination, HAB (n=12) and NAB (n=12) were tested in the rotarod test (4 days, 3 times per day for 300 s). When mice lost balance on the rotarod due to controlled acceleration (Figure 10a), they fell off the rod and the corresponding latency was recorded. In Figure 10 the mean latency (3 trials per day) is plotted for each animal (Figure 10b) and as a mean for all 12 NAB and 12 HAB mice (Figure 10c) during the 4 testing days (1, 2, 3 and 10). Regarding the mean latency, no significant differences were observed between HAB (red) and NAB (blue) mice (Strain:  $F(1, 22) = 1.239$ ;  $p=0.2777$ ; Days:  $F(3, 66) = 2.441$ ,  $p=0.0720$ ). The percentage of HAB and NAB mice that could manage to keep balance until the end (cut-off >300s), did not significantly differ between the two groups (Figure 10e;  $p=0.1952$ ). Comparing the cut-off-percentage across the trials, however, HAB tended to perform better on the accelerating rod (Figure 10d). It is of note, that HAB mice weighted significantly less ( $t=2.585$ ,  $df=22$ ;  $p=0.0169$ ) compared to NAB mice (Figure 10f).

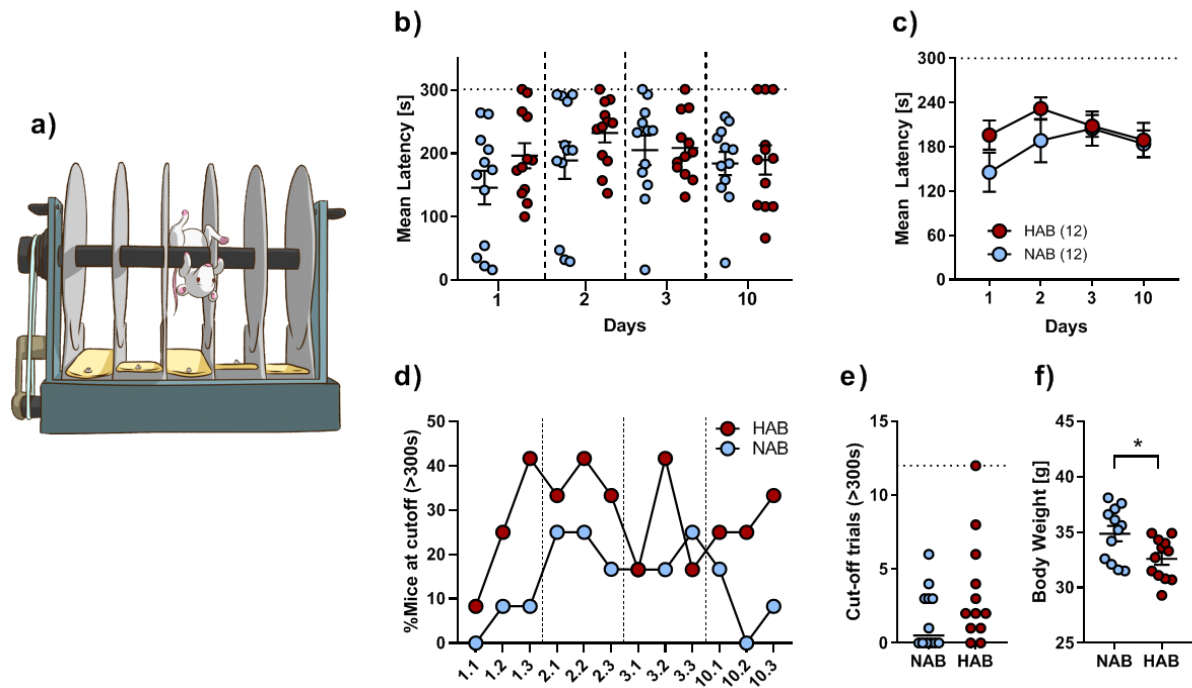


**Figure 10: No significant differences in rotarod performance between HAB and NAB mice.** Groups of HAB (n=12) and NAB (n=12) mice were tested. **(a)** Schematic illustration of the rotarod setup (Hamidi, 2015). **(b)** Mean latency [s] until falling down the accelerating (see Methods 2.3.1) rod [s] is shown per animal per day. **(c)** Groups mean latency [s] per day; **(d)** Percentage of mice performed for longer than 300 s on each trial; **(e)** Number of mice that performed longer than 300 s on each trial [trials]; **(f)** HAB (mean body weight: 32.6 g) mice were significantly lighter than NAB (mean body weight: 34.9 g) mice. \*  $p < 0.05$  (unpaired t-test).

### 3.2.2 HAB and NAB mice learned during the Detour Water Maze paradigm

After the rotarod test (3.2.1), mice underwent the detour water maze test assessing their cognitive flexibility (see Methods, Figure 5). On day 1 to 3 mice had to reach a visible, well-indicated platform, whereas on day 4 and 5 the platform was protected on the direct swimming path using a transparent barrier while mice had to reach the platform (cf. Figure 5). The escape latency of both groups, HAB (n=12) and NAB (n=12), decreased significantly about 40 s between the first and second day, whereas they stayed rather stable between 2-9 s at day 3 (Days:  $F(4, 88) = 52.07$ ,  $p < 0.001$ ; Figure 11a). No significant differences in latencies were observed between HAB and NAB mice (Strain:  $F(1, 22) = 0.8077$ ,  $p = 0.3785$ ; Strain x Days:  $F(4, 88) = 2.035$ ,  $p = 0.0964$ ; Figure 11a). The introduced barrier on day 4 led to increased latencies in both groups, which declined again at the consecutive day.

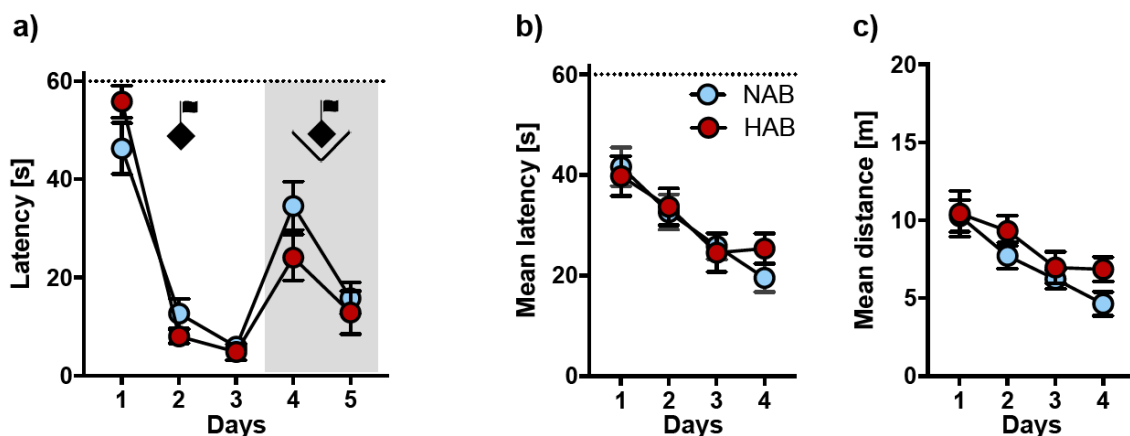


**Figure 11: Spatial learning and flexibility in HAB vs. NAB mice. (a)** HAB (red) and NAB (blue) mice showed no significant differences in their latencies reaching the platform during their first trials across 5 training days. On day 4-5 direct access to the platform was prevented by a transparent barrier. Mice had to reach the platform on an alternative path. **(b)** Mean latencies of all trials (4 per day) across the training days 1-4 in the Morris Water Maze. **(c)** Mean distance travelled throughout all trials across the training days 1-4.

### 3.2.3 HAB and NAB mice performed differently in the Morris Water Maze

After completing the Detour Water Maze paradigm, NAB and HAB mice (n=12 each) were tested in the Morris Water Maze test as a classical spatial learning protocol (see Methods, Figure 6). Performance was analyzed across the learning days (day 1-4). On day 5, a probe trial (PT) without the previous learned platform was performed and analyzed (cf. Figure 6). Figure 11b shows mean latencies of the trials across training days. Both, HAB and NAB showed reduced latencies over the consecutive training days (Day:  $F(3, 66) = 12.28, p < 0.0001$ ) with no differences between the two strains (Strain:  $F(1, 22) = 0.1271, p = 0.7248$ ; Strain x Day:  $F(3, 66) = 0.5547, p = 0.6468$ ). The same applied to the mean distance travelled (Figure 1c). Over the training days, both HAB and NAB mice travelled significantly shorter distances to reach the hidden platform (Day:  $F(3, 66) = 9.721, p < 0.0001$ ; Strain:  $F(1, 22) = 2.527, p = 0.1262$ ; Strain x Day:  $F(3, 66) = 0.4775, p = 0.6990$ ).

The training days were followed by a PT without the platform. The data analysis of the PT revealed that HAB mice spent significantly less time in the target quadrant (TQ=NW) compared to NAB mice (ANOVA Strain x Quadrant:  $F(3, 66) = 3.137, p = 0.0312$ ; Figure 12b), which is reflected by the heat maps of the probability of presence (Figure 12a). Moreover, HAB mice also travelled significantly less in the target quadrant compared to NAB mice (ANOVA Strain x Quadrant:  $F(3, 66) = 3.427, p = 0.0220$ ; Bonferroni's multiple comparisons test:  $p = 0.0144$ ; Figure 12c). Both groups, however, showed a preference for the TQ compared to the adjacent left (AL) and opposite quadrant (OQ). In general, both strains tended to stay closer to the learned platform position in the TQ, despite the higher proximity shown by NAB mice (Quadrant:  $F(3, 66) = 55.84, p < 0.0001$ ; Bonferroni's multiple comparisons test TQ:  $p = 0.0394$ ; Figure 12d). This is reflected by the increased number of platform crossings compared to virtual platform crossings in the three other quadrants (Figure 12e).

To investigate whether HAB and NAB mice show divergent behavior at various time points of the PT, the PT was analyzed in two equal periods of time (0 to 30 seconds and 30 to 60 seconds). Figure 12f-h indicates that NAB, but not HAB, intensified their search for the platform towards the end of the exposure ANOVA (Strain x Time:  $F > 3.760; p < 0.1123$ ).

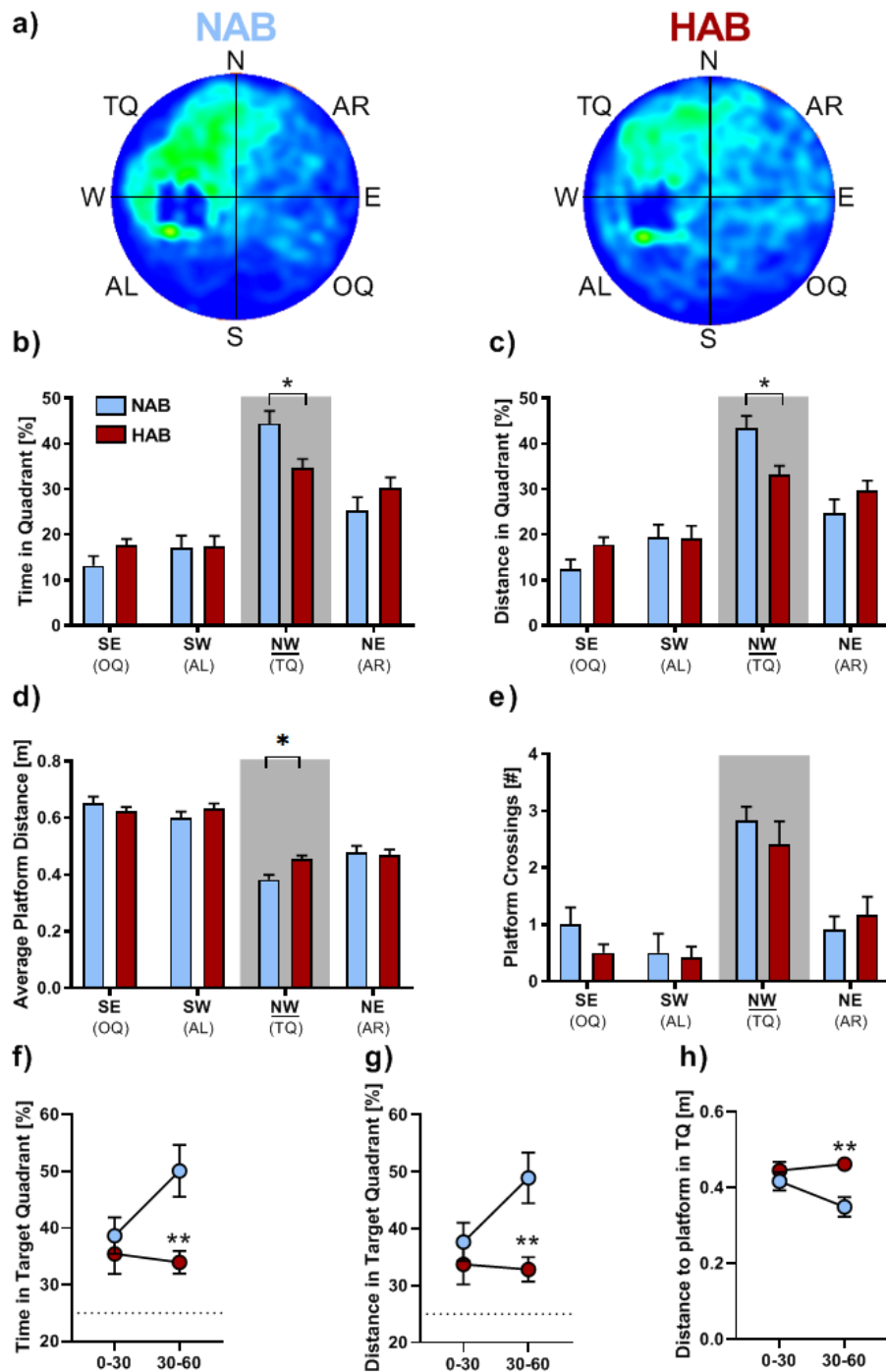


**Figure 12: Probe Trial (PT) at day 5 of the Morris Water Maze task. (a)** Heat maps illustrate the probability of presence of NAB (left) and HAB (right) mice; blue indicates less, green more presence at a location collapsed over all mice per strain. **(b-e)** Differences between HAB and NAB mice in (b) time spent, (c) distance travelled [expressed as percentage of total distance], (d) averaged platform distance and (e) platform crossings in the different quadrants. Opposite Quadrant OQ, adjacent left quadrant AL, target quadrant TQ, adjacent right quadrant AR. **(f-h)** PT analysis for the time periods of 0-30 s and 30-60 s. Differences between HAB and NAB mice in (f) time, (g) distance and (h) distance to platform in TQ. \*  $p < 0.05$ ; \*\*  $p < 0.01$  (two-way ANOVA followed by Bonferroni's multiple comparisons test).

### 3.3 Levels of synaptic density proteins – Molecular Correlates

To obtain insights into protein levels as molecular correlates for the volume differences detected using MRI, I focused on pre- and postsynaptic markers. To this end, I dissected the striatum (punched regions indicated by yellow circles in Figure 13a) and the dorsal hippocampus containing the CA3-regions (punched regions indicated by yellow circles in Figure 14a) from both hemispheres and performed a Western Blot analysis comparing HAB and NAB mice. Antibodies implicated in the maintenance of spines function are used: PSD-95 (95 kDa) followed by Synapsin (77 kDa), SynGAP (140 kDa) and GAP-43 (43 kDa). Expression levels were normalized to  $\beta$ -actin per mouse and expressed as percentage of the mean NAB levels.

#### 3.3.1 Striatum

In the striatum (Figure 13c) no significant differences in PSD-95 levels between HAB and NAB mice were observed ( $t=0.9861$ ,  $df=10$ ;  $p=0.3474$ ). In contrast, HAB mice showed significant less Synapsin ( $t=3.055$ ,  $df=10$ ;  $p=0.0121$ ) and SynGAP ( $t=2.478$ ,  $df=10$ ;  $p=0.0327$ ) compared to NAB mice (Figure 13d, e), whereas GAP-43 was enriched in HAB mice ( $t=2.422$ ,  $df=10$ ;  $p=0.0359$ ; Figure 13f).

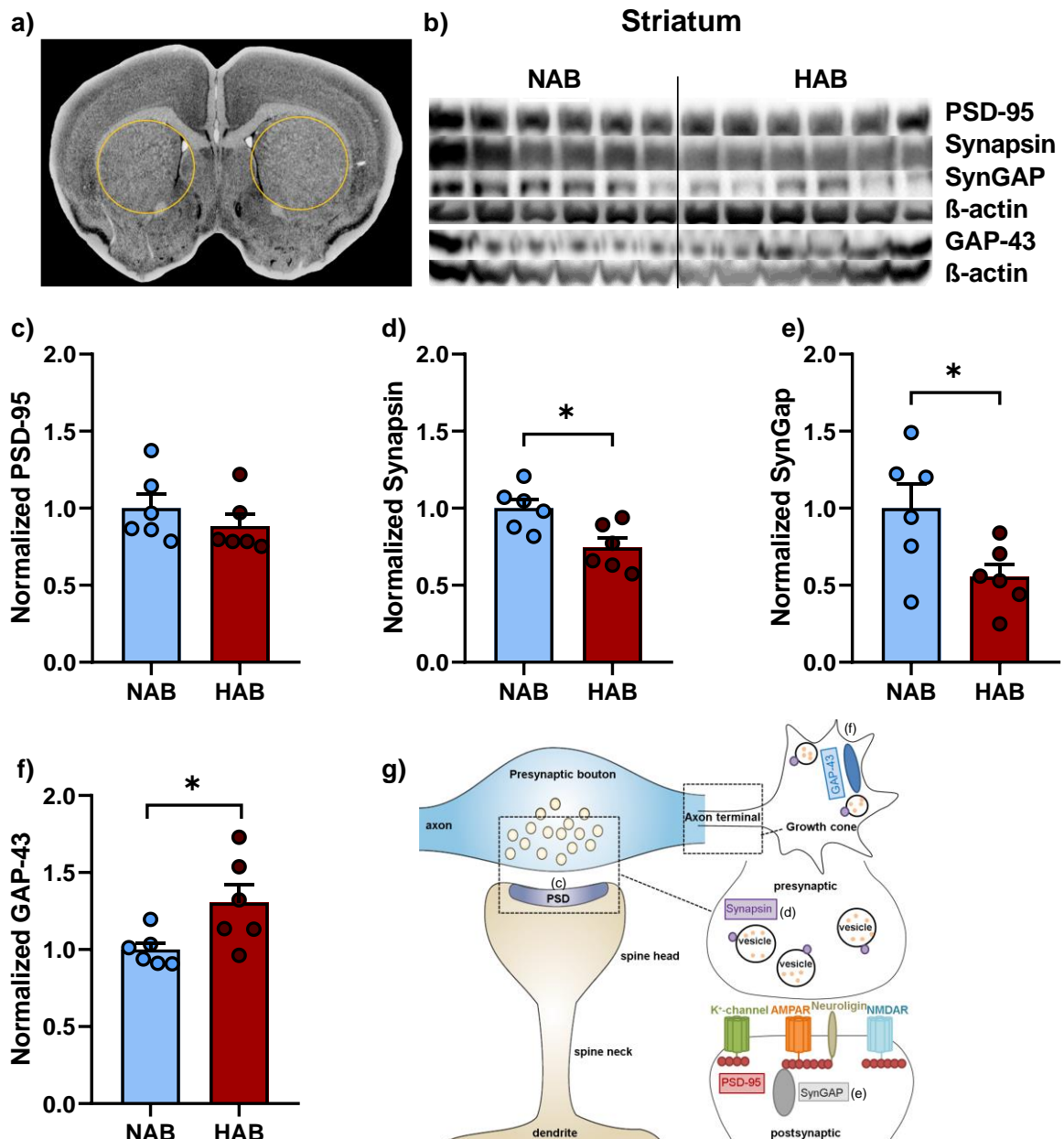


**Figure 13: Synaptic markers in the striatum of HAB vs. NAB mice.** (a) Punched regions were illustrated as yellow circles. (b) Western blot bands of PSD-95 (95 kDa), Synapsin (77 kDa), SynGAP (140 kDa) and GAP-43 (43 kDa) and the corresponding  $\beta$ -actin (45 kDa) of NAB and HAB mice are shown. (c-f) Band intensities were normalized to  $\beta$ -actin and to the intensities mean of the control condition (NAB). HAB mice were not different in their (c) PSD-95 levels, but levels of (d) Synapsin and (e) SynGAP were significantly lower compared to NAB. In contrast, the levels of (f) GAP-43 were significantly increased in HAB mice. (g) Putative localization of the investigated proteins in respect to presynaptic (axonal) vs. postsynaptic (dendritic) terminals. \*  $p < 0.05$  (unpaired t-test).

### 3.3.2 Hippocampus

Other than in the striatum, PSD-95 was significantly enriched in HAB compared to NAB mice ( $t=2.813$ ,  $df=10$ ;  $p=0.0184$ ; Figure 14c). No significant differences between the two groups were observed for Synapsin and SynGAP levels ( $t=1.768$ ,  $df=10$ ,  $p=0.1074$ ;  $t=0.1016$ ,  $df=10$ ,  $p=0.9211$ ; Figure 14d, e). GAP-43, however, is enriched in the CA3-region in HAB mice ( $t=2.364$ ,  $df=10$ ;  $p=0.0397$ ).

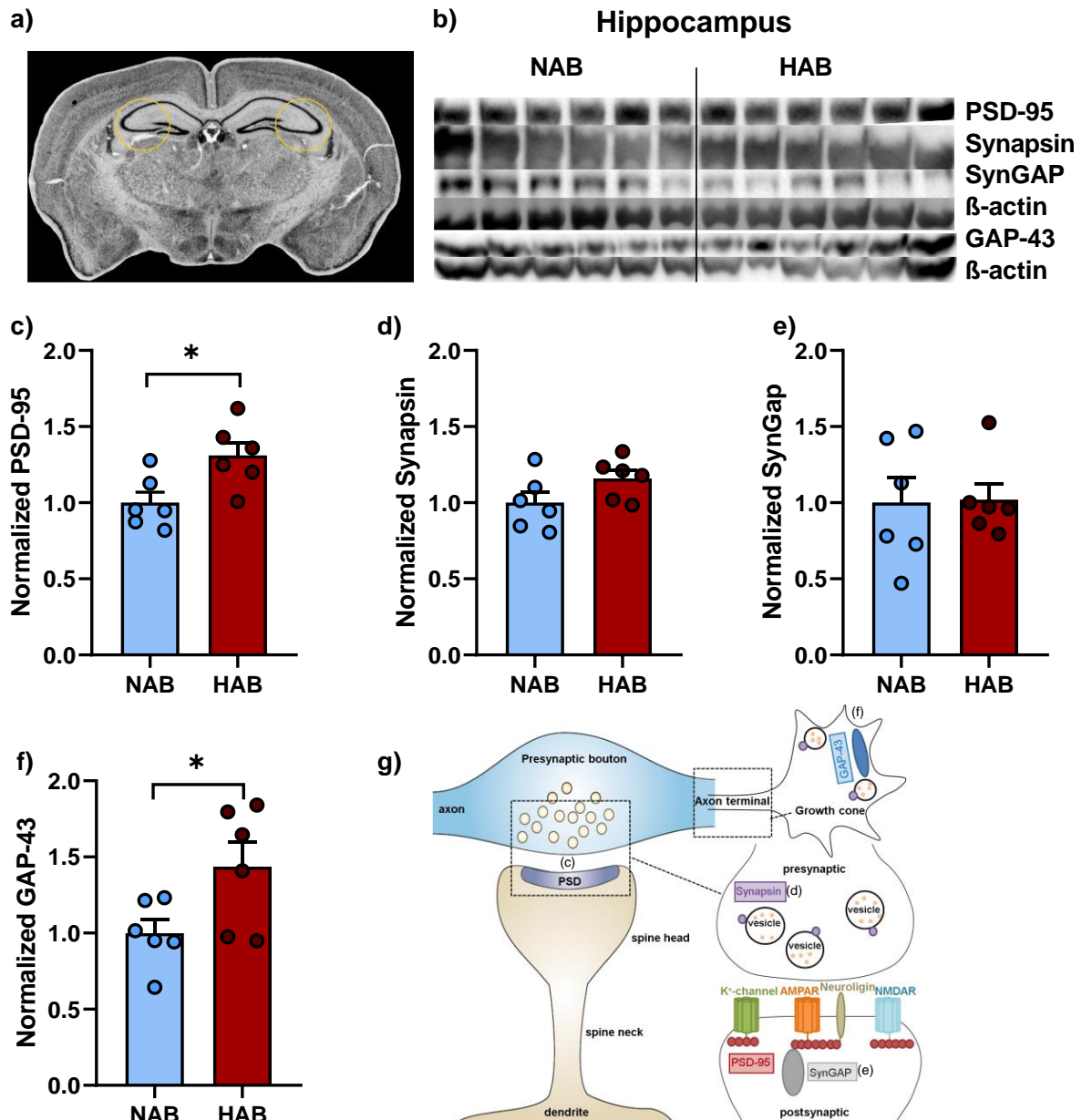


**Figure 14: Synaptic markers in the hippocampus of HAB vs. NAB mice.** (a) Punched regions were illustrated as yellow circles. (b) Western blot bands of PSD-95 (95 kDa), Synapsin (77 kDa), SynGap (140 kDa) and GAP-43 (43 kDa) and the corresponding  $\beta$ -actin (45 kDa) of NAB and HAB mice are shown. (c-f) Band intensities were normalized to  $\beta$ -actin and to the intensities mean of the control condition (NAB). HAB mice showed significantly increased (c) PSD-95 levels compared to NAB mice, but no differences in their (d) Synapsin and (e) SynGap levels were observed. Levels of (f) GAP-43 were significantly increased. (g) Putative localization of the investigated proteins in respect to presynaptic (axonal) and postsynaptic (dendritic) terminals. \*  $p < 0.05$  (unpaired t-test).

### 3.4 HAB mice show an increased spine density in the Striatum

To address the hypothesis that obtained differences in volume and spine protein levels could be ascribed to diverging quantities of spines, I performed a quantitative analysis of spines in striatal medium spiny neurons (MSNs) using Golgi impregnated brain sections (see Methods, cf. Figure 8).

The quantitative spine analysis revealed that HAB mice have significantly more spines per  $\mu\text{m}$  dendrite compared to NAB mice ( $t=5.977$ ,  $df=262$ ;  $p<0.0001$ ; Figure 15b), which is reflected if the mean values per animals were considered ( $t=2.670$ ,  $df=9$ ;  $p=0.0256$ ; Figure 15c). Next, I analyzed the number of spines across two segments which vary in their distance from the soma (Figure 15d). Segments further away from the soma ( $40\ \mu\text{m}$ ) have significantly more spines than the more proximal ones ( $20\ \mu\text{m}$ ) (Distance:  $F(1, 258) = 57.83$ ,  $p<0.0001$ ; Tukey's multiple comparisons test:  $p<0.0001$ ). Moreover, HAB mice showed more spines at both segments,  $20\ \mu\text{m}$  (Strain:  $F(1, 258) = 43.03$ ;  $p<0.0001$ ; Tukey's multiple comparisons test:  $p<0.0001$ ) and  $40\ \mu\text{m}$  (Tukey's multiple comparisons test:  $p<0.0001$ ), compared to NAB mice.

To compare spine densities for different compartments of the striatum, we assigned the randomly selected neurons used for analysis to either the dorsolateral (DL) or the dorsomedial (DM) striatum (Figure 15f). Spine densities were in general higher in the DM than in the DL part (Region:  $F(1, 260) = 12.47$ ,  $p=0.0005$ ). Again, HAB mice showed higher spine densities (Strain:  $F(1, 260) = 35.24$ ,  $p<0.0001$ ) irrespective of the region (Strain x Region:  $F(1, 260) = 0.1313$ ,  $p=0.7174$ ).

Due to intense staining effects in the hippocampus, it was not possible to perform spine analysis for this region (representative image: Figure 16).

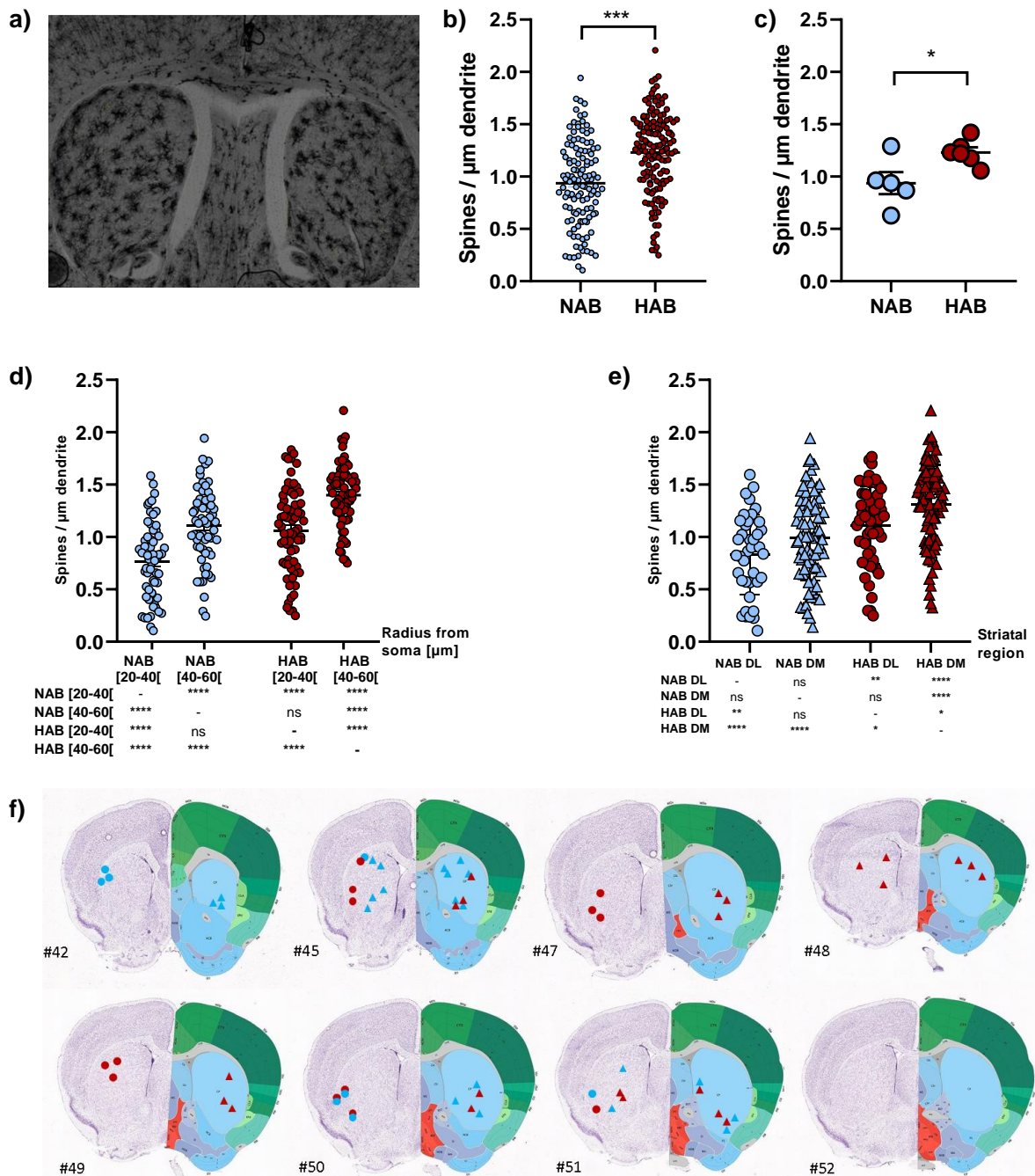


**Figure 15: Quantitative spine analysis of striatal medium spiny neurons. (a)** Representative image of a Golgi-stained striatal section. **(b-e)** Spine densities depicted (b) for individual segments (i.e. multiple data points per animal), (c) per animal (average of individual data points per mouse) and (d) irrespective of the distance from the soma and (e) striatal subregions. **(f)** Spatial distribution of selected striatal neurons for quantitative spine analysis (blue circles: NAB DL; blue triangle: NAB DM; red circle: HAB DL; red triangle: HAB DM). DL: Dorsolateral; DM: Dorsomedial; \*  $p < 0.05$ , \*\*  $p < 0.01$ , \*\*\*\*  $p < 0.0001$  (unpaired t-test, two-way ANOVA followed by Tukey's multiple comparisons test).

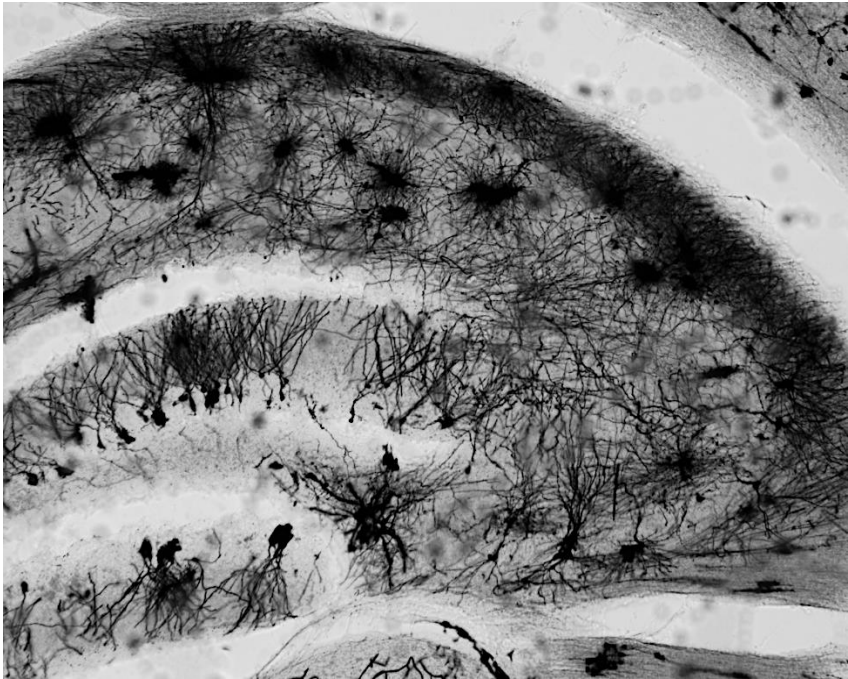


**Figure 16: Representative Golgi-stained hippocampal section.** Due to intense staining, spine analysis could not be performed in the hippocampus.

## 4 Discussion

Many patients suffer from generalized anxiety disorder (GAD), whereas little is known about the neural basis causing its pathology. The lack of knowledge always limits the potential of development of new therapeutics at one later stage. In my project I focused on the characterization of a well-established mouse model of GAD. High anxiety behavior (HAB) mice were selectively inbred based on their behavior shown on the EPM, interpreted as increased anxiety states. HAB mice show, compared to their controls, strong levels of anxiety and increased fear reactions in a variety of behavioral tasks (Krömer et al., 2005; Yen et al., 2012). Many attempts were taken to investigate the base of the manifested behavioral phenotype. Metabolic studies revealed different profiles between the trait anxiety strains (Filiou et al., 2014), whereas genetic approaches suggested a role of TMEM132E (Gregersen et al., 2014) as a potential regulating factor. In addition, microdialysis studies on neuropeptides and neurotransmitters were performed suggesting altered signaling of arginine vasopressin and GABA (Wigger et al., 2004; Tasan et al., 2011). In line with altered neuronal signaling, studies assessing basal neural activity using Manganese Enhanced MRI (MEMRI) were undertaken (Genewsky et al., 2018). Building on the observed changes in basal activities, I aimed to further characterize HAB and NAB mice on their GMV.

Using VBM I could demonstrate a reduced GMV in the striatum and the CA3-region of the hippocampus of HAB mice, which was partially supported by reduced synaptic markers in the striatum, but – unexpectedly – not by the number of spines.

## 4.1 Anxiety and Brain Volume

There are some approaches to determine the volume of the brain. One possibility is the extraction of the entire brain or defined regions of interest following by weighing them *ex vivo*. With the *in vitro* tissue sections and specific staining, the extracellular space can be visualized and analyzed. However, the limitations of the methods are a lack of accuracy with potential volume distortions due to invasive methods and fixation procedures and the unbiased whole-brain analysis is also not possible.

Therefore, in this project we conducted *in vivo* voxel-based GMV measurements using MRI. During the *in vivo* volume measurement, the brain remains in its native state with all its extracellular space, which may distort in *ex vivo* analyses. *In vivo* imaging can prevent artefacts caused by shrinkage effects, however, small artefacts caused by slight movements of the animal have to be prevented and/or corrected. One of the strongest advantages using *in vivo* MRI is the possibility to represent the total brain in single voxels, which, as a consequence, allows identifying regions which would not be considered in a biased, region of interest approach. The ventricular system as a part of the extracellular space, strongly contributes to the total brain volume and can be computed separately. Consequently, it is possible to exclude the ventricle volume from analysis, which results in a more proper reflection of the “real” GMV. Additionally, a high translational potential is given since *in vivo* MRI is feasible in man and mice. Findings from human subjects may be back-translated and studied in detail in distinct animal models. In my study, I had access to a 9.4 T animal MRI obtaining a resolution of 0.077x0.077x0.077 mm<sup>3</sup>. Two statistical thresholds were applied: an explorative one to detect minor changes in small regions and the FWE only showing strong changes. Comparing 9 HAB to 10 NAB mice, several brain regions seem to be different between the groups (see Results Figure 9). The following appear to be of particular interest: HAB mice showed a reduced volume in the striatum and the CA3-region of the hippocampus, whereas the triangular septal GMV was increased.

Results from MEMRI (Manganese Enhanced MRI) analysis (baseline, 8 injections, scan 24h after last injection, 7 T scanner) revealed that HAB mice show increased accumulation of Mn<sup>2+</sup> in the entire hippocampus (including CA3), the caudal part of the lateral septum and the interpeduncular nucleus (IPN) (see Figure 17; (Genewsky et al., 2018)). Given the fact that MEMRI research makes use of shared

physicochemical properties of  $\text{Ca}^{2+}$  and  $\text{Mn}^{2+}$ , it is coherent that  $\text{Mn}^{2+}$  can pass through ion channels similar to  $\text{Ca}^{2+}$  in an activity dependent manner and is thus used as a means of visualizing activity dependent changes in specific brain circuits (Wang et al., 2015). Following the permeation through  $\text{Ca}^{2+}$  channels,  $\text{Mn}^{2+}$  is transported along the axons and accumulates at their terminals (Wang et al., 2015; Bedenk et al., 2018).

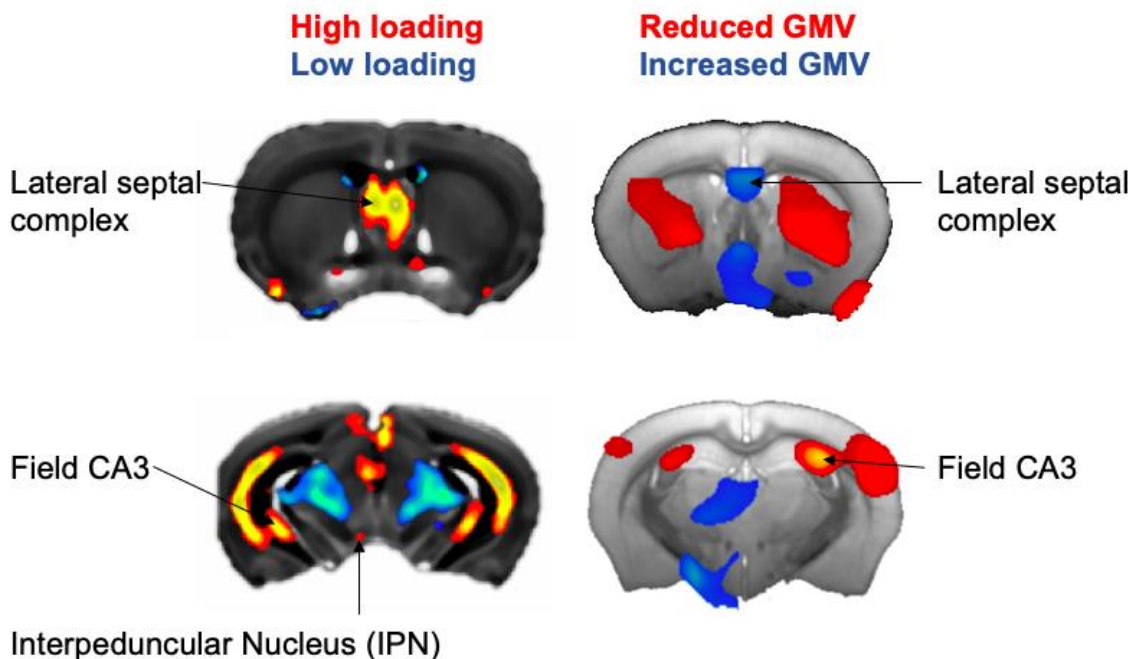


**Figure 17: Synopsis of MEMRI (left) and VBM (right) results:** neuronal brain activity (left) and GMV (right) of the lateral septum (LS)/triangular septum (TS) and the hippocampal CA3-region of HAB vs. NAB mice (redish colours: high loading and reduced GMV in HAB compared to NAB mice) (adapted from: Genewsky et al., 2018).

Considering the before mentioned results of MEMRI and VBM analysis, one linking hypothesis may be: The increased neuronal activity at level of the hippocampus leads to adaptive changes in GMV of the hippocampal CA3-region (HAB < NAB). One of the output structures of the CA3-region is the septum comprising a lateral, medial, and the posterior part which can be further subdivided into the triangular septum (TS) and the bed nucleus of the anterior commissure (BAC; (Yamaguchi et al., 2013). The increased neuronal activity of the CA3 causes increased  $\text{Mn}^{2+}$  accumulation in the septum (TS) and - in consequence - trophic effects at level of the TS (Figure 17). The TS serving as a crucial neural substrate controlling anxiety-

related behavior innervates the medial habenula (MHb) which, in turn, projects to the inter peduncular nucleus (IPN; (Yamaguchi et al., 2013). The efferent fibers originating in the IPN project to upper raphe nuclei, which in turn innervate the striatum, the prefrontal cortex, the extended amygdala and the amygdala-hippocampal complex which constitutes an important input structure to the MHb via the septum. This circuit is assumed to have regulating effects within the anxiety response system (Batalla et al., 2017). Remarkably, also the IPN shows enhanced  $Mn^{2+}$  accumulation (Figure 17), which is in agreement with an enhanced neuronal activity at level of the MHb, given the fact that  $Mn^{2+}$  is taken up in an activity-dependent manner (Bedenk et al., 2018) and accumulating towards the projection terminals (Wang et al., 2015; Almeida-Correa et al., 2018; Bedenk et al., 2018). All in all, this strongly supports the idea of chronically increased neuronal activity in the CA3 → TS → MHb → IPN pathway. Considering the involvement of the septohippocampal and septohabenular pathway in the modulation of anxiety (McNaughton and Gray, 2000; Yamaguchi et al., 2013; Parfitt et al., 2017) and of the MHb and IPN in the expression of aversive memories associated with anxiety (Soria-Gomez et al., 2015), it is tempting to speculate that this altered neuronal activity may explain, at least in part, the changes in anxiety-related behavior observed between HAB and NAB mice.

However, it is important to also address the limitations of *in vivo* brain volume measurements. Since the close proximity to the cryocoil and the fact that fluid-filled spaces could cause artefacts, regions located near the cortical surface and the ventricular system should be interpreted with caution. Given these facts, it should be considered that the CA3-region and the TS, but not the striatum, are located in close proximity to the lateral ventricle and thus, independent of the FWE, should be confirmed elsewhere. Due to technical (distorted images) and biological (mortality during anesthesia) reasons, we could only analyze 9 HAB and 10 NAB mice. My measurements will provide indications on an explorative base and are recommended to be further investigated at a molecular or morphological level which is only feasible in animal but not in human research.

## 4.2 Behavioral correlates for the regions of altered grey matter volume

### 4.2.1 Synaptic plasticity within the CA3-region of the dorsal hippocampus might contribute to the enhanced spatial precision of NAB mice

Following the observed changes in GMV between the strains, I focused on a behavioral characterization of the experimental groups. The CA3-region of the dorsal hippocampus – reduced in HAB mice – forms an auto-associative network memory system through three major converging afferents. Inputs to the CA3-region arrive from the dentate gyrus (DG) via mossy fibers, from the entorhinal cortex via the perforant path (pp) and from the recurrent collaterals of the CA3 pyramidal cells (Kesner, 2013; Rebola et al., 2017).

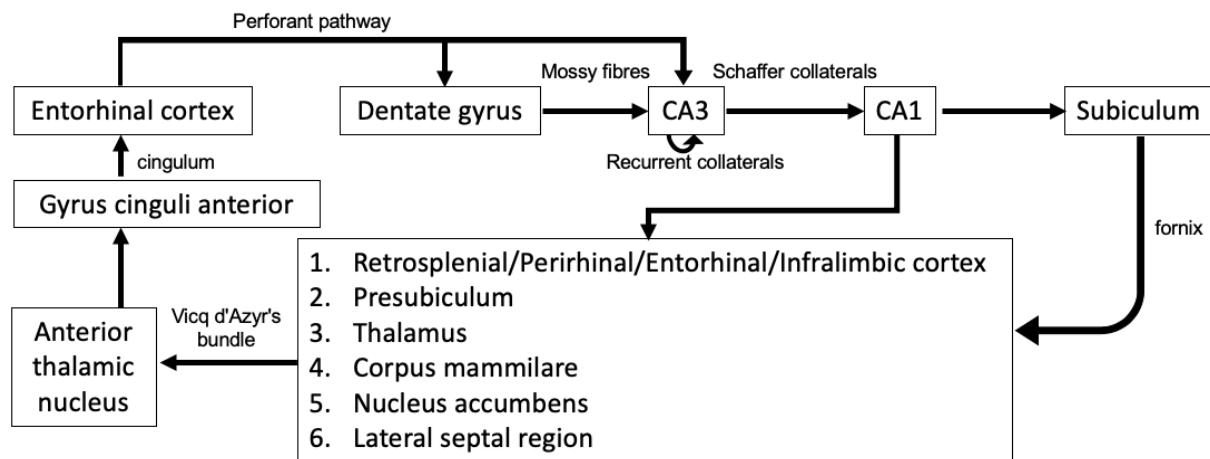


**Figure 18: Projections to, from and within the hippocampal formation** (adapted from: Andersen et al., 2007).

This network helps to initially store memories and the recurrent collaterals are subsequently involved in the recall of memory initiated only in presence of a fragmental cue of the same memory (Treves and Rolls, 1994; Rolls, 2007; Kesner and Rolls, 2015). By becoming associatively modified, hippocampal synapses are considered to be involved in learning and memory (Treves and Rolls, 1994; Martin et al., 2000; Morris, 2003; Rolls, 2007; Wang and Morris, 2010). While acting as a cognitive map (O'Keefe and Nadel, 1978), the entire hippocampus with its place cells exhibiting characteristic firing patterns in specific regions of space (the place field) and, therefore, is involved in spatial navigation (O'Keefe et al., 1998; Andersen et al., 2007).

The Detour Water Maze is a paradigm to test for cognitive flexibility by introducing a transparent barrier that has to be bypassed to reach the platform. Inducing a discrepancy between the visual stimulus, seeing the platform, and the tactile/motoric perception to not reach the platform force mice to show a flexible bypass (Juszczak and Miller, 2016). As HAB and NAB mice showed no significant differences in their latencies to reach the platform, obviously both lines are able to exert cognitive flexibility. Although the hippocampus is needed during the navigation, the capability of inhibiting processes has been ascribed to the prefrontal cortex (Diamond, 1990; Maguire et al., 1998; Spiers and Gilbert, 2015; Kabadayi et al., 2018). By the fact that mice reached the visual (marked by a flag) platform in under 20 s (see Figure 11a), the task might be too simple. One aggravating condition would be to rotate the barrier 180 degrees which further complicates the finding of the platform. Another alternative is the performance of the more challenging Morris Water Maze as a classical spatial learning and reference memory paradigm (Morris, 1984; Vorhees and Williams, 2006).

The Morris Water Maze is frequently used to test hippocampal-dependent spatial learning performance. However, studies revealed the strong input of also many other brain structures like the superior colliculus (visual perception), nucleus accumbens (motivation), posterior parietal cortex and others (Garthe and Kempermann, 2013). Comparing HAB and NAB mice during the hidden platform training, they showed no differences in their latencies nor their distances travelled to reach the platform. The hippocampus seems to play a minor role in general learning processes but a greater role in precision of learning and memories (Ruediger et al., 2011). To investigate the searching strategies of HAB and NAB mice, the probe trial (PT), without the presence of the hidden platform, was performed and analyzed subsequently. The PT analysis revealed that HAB compared to NAB mice spent less time and swam shorter distances in the TQ and showed a generally lower proximity to the target platform location (see Results, Figure 12). This indicates a less precise searching strategy of HAB compared to NAB mice.

Explaining the different performance in the PT, a potential panic-like behavior of HAB mice, that may lead to a divergent emotional state once they realized the absence of the “save” escape platform, needs to be considered. This should be reflected in the dynamics of the selective searching strategies, and with this, in the passage of time.

However, the analysis across time (0 to 30 s and 30 to 60 s) revealed a stable performance of HAB mice across the entire exposure (see Results, Figure 12f-h), whereas the searching strategy of NAB mice improved and became more precise.

Chronic stress has previously been shown to impair spatial and hippocampus-dependent learning (Luine et al., 1994; Conrad et al., 1996). HAB mice, described as a model of GAD may be exposed to repeated, or even chronic stress through the high emotional load. In line with this, HAB rats are known to exhibit stronger responses to weak stressors indicative of their increased vulnerability to stress (Landgraf and Wigger, 2003; Landgraf et al., 2007). In addition to the chronic, the acute emotional component of high anxiety behavior in HAB mice needs to be considered.

Thus, memory performance of HAB mice need not necessarily be affected by their anxious behavior, the chain of causality, however, may be present: the CA3-region of the hippocampus, a region crucially implicated in spatial learning and memory processes, shows structural plasticity in response to spatial learning (Ramirez-Amaya et al., 1999; Ramirez-Amaya et al., 2001). Following chronic stress, animals show a reduced hippocampal GMV as well as a loss of synapses within the CA3-region of the hippocampus (Sousa et al., 2000). The altered GMV might be understood as a protective reaction towards stress. As a result of stress, high cortisol levels lead to dendritic retraction in the hippocampus to reduce the contact surface (Dias et al., 2014). Consequently, neurons are damaged leading to reduced hippocampal volume and thereby to memory impairment (Moon and Jeong, 2017). Moreover, it was previously shown that stress modulates synaptic plasticity in the hippocampus (Andersen et al., 2007). High level of stress accompanied by high corticosteroids levels impairs hippocampal LTP and – as a consequence – spatial working memory (Foy et al., 1987; Diamond et al., 1996; Kim et al., 1996; de Quervain et al., 1998).

This chain of causality might explain the deficit in accuracy during the probe trial of HAB mice, assuming them as stressed animals with an reduced GMV in the CA3-region of the hippocampus, a key region for spatial navigation and learning (Luine et al., 1994; Conrad et al., 1996).

The fact that both HAB and NAB mice have learned, endorsed intact motivation and locomotor capabilities and, in particular, a quality of sensory in- and outputs,

especially after Genewsky et al. (Genewsky et al., 2018) demonstrated strong visual deficits of low anxiety behavior (LAB) mice.

Whereas LAB mice were also known to be hyperactive, in-water-locomotion of NAB and HAB was not affected (see Results, Figure 11) in our experiments. However, to see whether HAB and NAB mice differ in their general basal activity it would be of interest for future studies to investigate their home cage activity. These results might support the theory that less activity also leads to less brain activity, which in turn results in reduced brain volume. In addition, given a constant learning curve (see Results, Figure 11) and the lack of any floating behavior, which would be interpreted as a lack of motivation to escape (Vorhees and Williams, 2006), mice were motivated to escape.

In summary it can be concluded that the decreased CA3 volume of HAB correlates with the performance accuracy during the probe trial and could most likely be explained by synaptic plasticity and its impact on memory processes. Cause and causality of the decreased CA3 volume, however, needs to be studied further.

### **4.2.2 The rotarod test may not be the proper task to represent the volume differences between HAB and NAB mice**

Next to the CA3-region, the striatum is decreased in HAB compared to NAB mice, too. Although recent studies of anxiety have been focused on many other structures like the amygdala or the hippocampus (HPC), the striatum has not been considered in playing a crucial part in the underlying mechanism despite existing anatomical and functional interactions (Calhoon and Tye, 2015; Lago et al., 2017).

The striatum, a nucleus of the basal ganglia, can be divided into a ventral and a dorsal part based on function and integration into striatal circuits. Whereas the ventral part of the striatum is involved in behavioral sensitization and Pavlovian learning (Dang et al., 2006), the dorsal striatum, based on the origin of their cortical afferents (association vs. sensorimotor cortices), is involved in cognitive and sensorimotor action control. This, in turn, can be subdivided into a dorsomedial (associative) and a dorsolateral (sensorimotor) part (Dias-Ferreira et al., 2009; Yin et al., 2009). The dorsomedial part of the striatum mediates goal-directed learning and is thereby involved in forming the associations between actions and their values of

outcome (Yin et al., 2005). In contrast, the dorsolateral part plays a role in forming the associations between a response and the preceding stimuli thus mediating habitual behavior (Yin et al., 2006). In general, the whole striatum is well known for its role in motor learning and reward-dependent decision-making processes (Balleine and O'Doherty, 2010). With the rotarod test, I focused on motor coordination and motor learning.

The rotarod protocol is commonly used in research fields dealing with disorders of severe impairments within the nigrostriatal pathways like Huntington's or Parkinson's Disease (Carter et al., 1999; Costa et al., 2004; Assaf and Schiller, 2018). HAB and NAB mice showed similar latencies in the rotarod task and performed relatively well in comparison to rotarod latencies shown in other studies of both, healthy (Scholz et al., 2015; Jurado-Arjona et al., 2019) mice. HAB mice tended to perform better when comparing the cut-off percentages across the trials, however, they weigh significantly less than NAB (mean body weight: 34.9 g). A lower body weight of HAB mice (mean body weight: 32.6 g) could allow for a better performance and might correlate with higher levels of basal movements in their home-cage.

The rotarod task might be too simple for both strains to represent the observed GMV deficits in HAB mice. The testing of goal-directed and habitual behavior (using tests like outcome devaluation and contingency degradation) may be a next step.

### **4.3 Potential cellular and molecular correlates of GMV changes in HAB mice**

#### **4.3.1 An interpretation of the hippocampal western blot results would require valid quantitative spine analysis for the hippocampus.**

The hypothesis that enhanced anxiety leads to a hypotrophy of hippocampal neurons was affirmed by Vyas et al. who identified chronic immobilization stress as a cause of dendritic remodeling in hippocampal neurons. The authors found that chronic immobilization stress induces a dendritic atrophy in hippocampal CA3 pyramidal neurons (Vyas et al., 2002). A detailed analysis revealed the shrinkage of apical dendrites of CA3 pyramidal neurons and a loss of synaptic spines, which is interpreted as a stress coping strategy (Watanabe et al., 1992; Conrad et al., 1999;

Lee et al., 2009). Stress associated with high cortisol levels lead to dendritic retraction in the hippocampus to reduce its contact surface consequently leading to reduced hippocampal volume (Dias et al., 2014).

Taking into account that the GM of mammals consists of about 30-35 % of synapses and dendrites (Bennett, 2011; Kassem et al., 2013), I primarily focused on them to investigate the reduced GMVs in HAB mice using morphological analysis: the Golgi Staining. By visualizing dendrites and spines, I quantified spines in the striatum, however, the staining of the hippocampal sections was too intense to proceed with a proper analysis.

PSD-95, increased in HAB mice, is a key protein of excitatory glutamatergic synapses and involved in synaptic transmission and plasticity by anchoring glutamate receptors like NMDA (Hering and Sheng, 2001; Kim and Sheng, 2004; Beique et al., 2006) in the postsynaptic density. NMDA receptors are known to be implicated in anxiety related disorders (Salunke et al., 2014), what is reinforced by the fact that NMDA receptor antagonists are able to reduce anxiety (Barkus et al., 2010). Given these facts, one explanation for increased PSD-95 levels in HAB mice might be: Anxiety lead to an increased glutamatergic tone in the hippocampus, like it was previously reported for restraint stress in rats (Gilad et al., 1990; Sunanda et al., 1995). This in turn, would require the involvement of NMDA receptors and, thus, PSD-95 as their linking structure. The enhanced activity of the glutamatergic system including NMDA receptors might be accompanied by the simultaneous adaption of PSD-95 towards increased levels as observed in HAB mice.

Another protein which shows enhanced levels in HAB mice is GAP-43, playing a major role in axonal outgrowth, synaptogenesis and synaptic remodeling (Morita and Miyata, 2013). Moreover, in response to neuronal damage GAP-43 is implicated in nerve sprouting (Grasselli and Strata, 2013). Thus, the increase of GAP-43 protein levels in HAB mice could be understood as a mechanism to compensate their reduced hippocampal volume which is most likely accompanied by neuronal damage. While previous studies described an association between GAP-43 expression and improved spatial learning along with LTP (Latchney et al., 2014; Su et al., 2019), we could not confirm these findings. In our study, HAB mice showed higher GAP-43 levels, but reduced accuracy in the PT of the MWM. A possible explanation might be the specific western blot analysis of the hippocampal CA3-region instead of including the entire hippocampus. Whether enhanced GAP-43 levels could also be associated

with increased hippocampal synaptogenesis would require a quantitative spine analysis within the hippocampus.

Beside spines, also other components of the GMV possibly contribute to volume differences between HAB and NAB mice. For instance, glial cells like oligodendrocytes or astrocytes might have a slight impact on the GMV. In addition, the hippocampus is located near the lateral ventricles what could lead to artefacts in the VBM-analysis, and therefore to delusive conclusions.

Nevertheless, a conclusive interpretation of the hippocampal western blot results would largely benefit from a valid analysis including spines' quantity and dendrites' length in the hippocampus, what makes further investigations necessary.

### **4.3.2 Increased spine density, reduced striatal GMV and spine markers in HAB mice – a compensation?**

As already observed in the hippocampus, striatal western blot results revealed increased protein levels of GAP-43, but also a reduction of SynGap and Synapsin protein levels in HAB mice. Considering the mentioned involvement of GAP-43 in synaptogenesis (see 4.3.1), increased protein levels would match with the increased number of spines in the striatum of HAB mice.

SynGap, a protein highly expressed at the PSD of excitatory synapses (Kim et al., 1998) was reduced in HAB mice. Through the trafficking of glutamate receptors to synapses, SynGap is known to be involved in LTP (Krapivinsky et al., 2004; Yang et al., 2013; Araki et al., 2015). Coinciding with the reduced SynGap levels, also Synapsin, a presynaptic phosphoprotein is less abundant in HAB mice. Synapsin is implicated in the release of synaptic vesicles and, thus, neurotransmitters, and following involved in neuronal plasticity and neuronal growth (Greengard et al., 1993; Cesca et al., 2010; Nikolaev and Heggelund, 2015). The reduction of spine markers including SynGap and Synapsin within the striatum of HAB mice suggest a decreased synaptic activity in the same region. This would be in line with the reduced striatal GMV of HAB mice, possibly caused by a loss of dendritic arborization. To see, whether these plastic changes are in accordance with low striatal activity and thus with behavioral deficits, further behavioral assessments of the striatum need to be performed.

To test the hypothesis, whether alterations in volume and spine protein levels might be ascribed to different spine quantities, I performed a quantitative spine analysis in striatal medium spiny neurons on Golgi impregnated brain sections. The analysis revealed that HAB mice have more spines per  $\mu\text{m}$  than NAB mice which is also reflected in the mean values per animal. Additionally, segments further away from the soma ( $40\ \mu\text{m}$ ) have significantly more spines than the more proximal ones ( $20\ \mu\text{m}$ ), whereby HAB mice showed more spines at both segments than NAB mice. In the DM part of the striatum, spine densities were in general higher than in the DL part and again, HAB mice showed higher spine densities irrespective of the region. The increased number of striatal spines in HAB mice might be associated with higher rates of synaptic transmission and enhanced activity. This might facilitate the anxious behaviors due to the striatum's involvement in anxiety mediating processes (Lago et al., 2017). The increased number of spines within in the volume-reduced striatum strongly suggest a compensatory mechanism according to which dendritic atrophy needs more synapses to gain a similar functional state. Dias et al., for instance, revealed that high-conditioned freezing rats, another animal model of GAD, show reduced dendritic trees within hippocampal structures, whereas the spine expression was increased (Dias et al., 2014). However, we cannot completely rule out that the increased number of spines may result from shrinkage processes within the striatum. The observed reduced striatal GMV in HAB mice might be a consequence of neuronal contraction, leading to a higher spine density along shrunken dendrites. To verify this hypothesis, it is indispensable to determine the dendritic length. This knowledge would allow a final interpretation of the spine analysis results either in the direction of compensatory or shrinking effects.

#### **4.4 Human equivalences**

Since in my project I mainly focused on the striatum and the hippocampus in mice, I will address the structures equivalent to these in humans to be able to transfer insights from animal to human research.

As an input nucleus for the cortico-basal ganglia circuitry the human striatum comprises the dorsal striatum with the caudate nucleus and the putamen (linked

together through the fundus), the ventral striatum consisting of the nucleus accumbens and the ventromedial aspects of the caudate nucleus and the putamen (Grahn et al., 2009; Marchand, 2010; Lago et al., 2017). The dorsal striatum receives projections from the prefrontal and parietal cortices and contributes to cognitive processes like decision making, action-initiation and motor functions (Porter et al., 2015; Lago et al., 2017). The ventral striatum receives inputs from the amygdala, the hippocampus, the medial orbitofrontal and anterior cingulate cortices and is involved in motivation as well as learning processes (Porter et al., 2015; Lago et al., 2017). Being involved in cortico-striatal-thalamic-cortical circuits the striatum is critically implicated in elementary behavioral processes that also play a major role in anxiety like attention, conditioning and motivation (Lago et al., 2017). This striatal involvement raises the question, whether there are striatal volume changes described in patients suffering from anxiety disorders. Indeed, several studies have revealed striatal GMV changes in patients with anxiety disorders. Hilbert et al., Liao et al. and Bas-Hoogendam et al. found an increased GMV in both, the right striatum of GAD patients (Liao et al., 2013; Hilbert et al., 2015) and the dorsal striatum of social anxiety disorder patients (Bas-Hoogendam et al., 2017). However, in HAB mice, the GMV was decreased in the striatum as it has previously been reported for major depressive disorder, consistent with decreased activation to rewarding stimuli of depressed patients (Kempton et al., 2011; Bora et al., 2012). At this point one has to consider that HAB mice are most likely an animal model for generalized anxiety disorder, but nevertheless comorbidity cannot be ruled out. In fact, GAD is known as a predictor for the development of major depressive disorder (MDD) which is often seen as a comorbid disorder (59%; Carter et al., 2001; Wittchen, 2002). Regardless of how, the striatum seems to play a role in pathologic anxiety.

The second structure I want to address is the hippocampus, which is located in the medial temporal lobe of the human brain. The bulb-shaped hippocampal formation protruding into the lateral ventricles comprises the brain areas of the dentate gyrus, the hippocampus with its subfields CA1-4, the subiculum, the presubiculum, parasubiculum and the entorhinal cortex (Andersen et al., 2007). Afferent projections, among others, arrive at the hippocampus from the brain stem (locus coeruleus, raphe nuclei), the thalamus and subcortical structures (septal nuclei; Andersen et al., 2007). The output projection to the mammillary body (hypothalamus) is the beginning of the Papez circuit which proceeds through the thalamus to the parahippocampal gyrus

and back to the hippocampal formation (see Figure 18). This neural loop is implicated in emotional experiences and the consolidation of memory (Papez, 1995; Choi et al., 2019). Beside its role as an integrator of emotion and cognition, the hippocampus is involved in learning, spatial navigation and memory storage and retrieval in connection with several cognitive functions (Treves and Rolls, 1994; O'Keefe et al., 1998; Martin et al., 2000; Morris, 2003; Rolls, 2007; Wang and Morris, 2010; Femenia et al., 2012; Moon and Jeong, 2017). In fact, Moon and Jeong found that patients with memory dysfunction and low attention, representing typical symptoms of GAD, also showed reduced GMV in the hippocampus as a morphological correlate (Moon and Jeong, 2017). Consistent with my findings of HAB mice, also human neuroimaging studies produced the same results of reduced hippocampal GMV in GAD patients (Hettema et al., 2012; Abdallah et al., 2013; Moon et al., 2014). These overlapping findings of underlying neurobiological processes (construct validity) might affirm HAB and NAB mice as an appropriate animal model for GAD.

To sum it up, results from human neuroimaging studies revealing increased striatal, but reduced hippocampal GMV in GAD patients. This partially match with my results of reduced striatal and hippocampal GMV in HAB mice. Animal research on the field of anxiety aims a better understanding of the underlying causes to finally let patients suffering from anxiety disorders benefit. However, it is of note that human beings are inhomogeneous individuals (grown up under various influencing conditions) demanding caution when translating findings from animals (consistent breeding conditions and equal genes) to human research.

## 5 Summary and Outlook

To conclude, with my thesis I found that extremes in trait anxiety (HAB) coincide with GMV alterations in specific brain structures, which I evaluated in its behavioral phenotypes and underlying molecular signature.

In the first part of my study I conducted *in vivo* GMV measurements of HAB and NAB mice using MRI. Unbiased, VBM analysis of the entire brain revealed a decrease in the CA3-region of the dorsal hippocampus and the striatum, whereas the triangular septum (TS) was increased in HAB compared to NAB mice. These findings are along with a previous study showing altered activity in at least parts of the mentioned structures. Increased neuronal activity in the hippocampus may cause adaptive GMV changes, not only at the level of the hippocampus but, due to its projections to the TS, also lead to trophic effects within the TS. Given the fact that the IPN in HAB mice also showed increased brain activity, supports the idea of increased neuronal activity within the CA3 → TS → MHb → IPN pathway, providing a potential explanation for the observed differences between HAB and NAB mice (Genewsky et al., 2018). Hence, it would be of interest to investigate this circuitry in HAB mice in more detail by applying methods like investigating activity patterns by c-Fos expression combined with tracing the pathway by the use of antero- and retrograde viral approaches. This would be followed by a functional validation by inhibiting or enhancing parts of the hypothesized pathway using opto- or chemogenetics.

The next part aimed at the potential correlation between altered brain structures and their involvement in specific functions. Therefore, hippocampal and striatal-dependent processes were assessed in behavioral procedures.

The detour paradigm, potentially involving the hippocampus and the prefrontal cortex, should verify the ability of cognitive flexibility (Diamond, 1990; Spiers and Gilbert, 2015). As HAB and NAB mice showed no significant differences in their detour performances, obviously both lines are able to exert a basic cognitive flexibility. With regard to the obtained latencies the task may be too simple. In future studies it would make sense to rotate the barrier 180° to aggravate the conditions to possibly reveal strain differences.

As a more complex hippocampal-dependent behavioral test I performed the MWM, a classical paradigm to test spatial learning and memory (Morris, 1984; Vorhees and Williams, 2006). NAB compared to HAB mice searched more precisely during the PT. It is known that stress associated with high levels of cortisol causes loss of synapses which might explain the reduced hippocampal volume observed in HAB mice (Sousa et al., 2000). Moreover, LTP and spatial memory are impaired as a result of stress which might serve as an explanation for the accuracy deficits of HAB mice (Foy et al., 1987; Diamond et al., 1996; Kim et al., 1996; de Quervain et al., 1998). Therefore, it would be of interest for future studies to perform hippocampal LTP and LTD measurements using VSDI (voltage-sensitive dye imaging) in HAB and NAB mice to confirm this hypothesis (Stepan et al., 2012). In addition, other spatial working memory tasks, as the complex Atlantis platform task, could be performed. With the advantage of reducing the chance-finding by replacing the hidden platform with a collapsible one, the Atlantis platform task would reflect the use of mapping strategies combined with a high degree of cognitive flexibility (Buresova et al., 1985; Spooner et al., 1994).

In a next step, I assessed striatal-dependent processes playing a major role in motor learning and reward-dependent-decision making (Balleine and O'Doherty, 2010). Therefore, mice were tested on the rotarod test, which focusses on motor coordination and learning. The lower body weight of HAB mice might explain the lack of differences in the rotarod performance. At this point, it would be interesting whether the lower body weight values stem from higher levels of basal movements. This could be confirmed by measuring the home cage activity (e.g. Genewsky et al., 2017) which would prove the hypothesis that low levels of locomotor activity associated with reduced striatal activity, resulting in reduced GMV. The good performance of HAB and NAB mice relative to other studies suggests that the rotarod task might be too simple to represent the striatal GMV deficits of HAB mice. Future tries to test striatal-dependent processes would comprise both, assessing more motivational processes with an additional learning component using for example the progressive ratio-touchscreen protocol (Horner et al., 2013) or, as a fine-motor skill task, performing the grasping experiment (Tucci et al., 2007).

As a third morphological approach, I performed western blot procedures and quantitative spine analysis on Golgi stained brain sections. As the staining in the hippocampus was too intense, the spine analysis was only feasible for the striatum. Anxiety might lead to an enhanced glutamatergic tone involving an increase of NMDA receptors, which are anchored to the PSD through PSD-95 (increased in the hippocampus of HAB mice). Among other functions like axonal outgrowth and synaptogenesis, GAP-43 is implicated in nerve sprouting (Grasselli and Strata, 2013). Thus, increased levels of GAP-43 in HAB mice might be seen as a mechanism to compensate their reduced hippocampal volume associated with neuronal damage. A quantitative spine analysis in the hippocampus would be essential for associating enhanced GAP-43 levels with increased hippocampal synaptogenesis. An additional validation of the protein levels using different breeding stocks (like Innsbruck (Singewald-Lab) or Regensburg (Neumann-Lab)) would, concerning a potential genetic drift, strengthen its validity. Since the genetic variation and its related phenotype changes randomly (stochastic) over time, the gene pool of HAB and NAB mice might be divergent in the different laboratories (separated since 2003). Moreover, the understanding of underlying causes leading to different behavior shown by HAB mice would benefit from performing the statistical analysis of quantitative trait locus (QTL). By linking information about the genotype (single nucleotide polymorphisms (SNP)) and its complex phenotypic trait (anxiety), QTL analysis aims at determining molecular regions underlying the phenotypes (Abiola et al., 2003; Landgraf et al., 2007).

In the striatum, protein levels of GAP-43 were increased, whereas the protein levels of both SynGap and Synapsin showed reduced levels in HAB mice. Given the involvement of GAP-43 in synaptogenesis, the increased protein levels could be brought in line with the increased striatal spine number in HAB mice. The reduced striatal level of SynGap and Synapsin which are implicated, among others, in neuronal plasticity (SynGap and Synapsin) and neurotransmitter release (Synapsin) might underly reduced synaptic activity in the same region. This, in turn might be consistent with the reduced striatal GMV of HAB mice. However, additional, sophisticated striatum-dependent behavioral tasks may be recommended.

A last open issue is the increased spine number of HAB mice. This could be interpreted as a compensation for atrophied dendrites within the reduced striatum, or rather results from shrinking effects causing an increased spine density along the

shrunk dendrites. Measuring the length of the same dendrites on which I counted the spines could address this issue.

Taken together, my findings, especially on the reduced hippocampus hold an increased translational value since GAD patients exhibit a similar trophism. Back-translating and unveiling underlying anxiety mechanism may contribute to a better understanding and treatment of anxiety disorders.

## Bibliography

- Abdallah CG, Coplan JD, Jackowski A, Sato JR, Mao X, Shungu DC, Mathew SJ (2013) A pilot study of hippocampal volume and N-acetylaspartate (NAA) as response biomarkers in riluzole-treated patients with GAD. *European neuropsychopharmacology : the journal of the European College of Neuropsychopharmacology* 23:276-284.
- Abiola O et al. (2003) The nature and identification of quantitative trait loci: a community's view. *Nature reviews Genetics* 4:911-916.
- Almeida-Correa S, Czisch M, Wotjak CT (2018) In Vivo Visualization of Active Polysynaptic Circuits With Longitudinal Manganese-Enhanced MRI (MEMRI). *Frontiers in neural circuits* 12:42.
- American Psychiatric Association (2013) *Diagnostic and Statistical Manual of Mental Disorders, Fifth Edition*. Arlington, VA: American Psychiatric Association Publishing.
- Andersen P, Morris R, Amaral D, Bliss T, O'Keefe J (2007) *The Hippocampus Book*. Oxford, New York: Oxford University Press. p.: 3, 12, 38, 108-109, 512-513, 757-760
- Andlin-Sobocki P, Wittchen HU (2005) Cost of anxiety disorders in Europe. *European journal of neurology* 12 Suppl 1:39-44.
- Araki Y, Zeng M, Zhang M, Hagan RL (2015) Rapid dispersion of SynGAP from synaptic spines triggers AMPA receptor insertion and spine enlargement during LTP. *Neuron* 85:173-189.
- Assaf F, Schiller Y (2018) A chemogenetic approach for treating experimental Parkinson's disease. *Movement disorders : official journal of the Movement Disorder Society*.
- Balleine BW, O'Doherty JP (2010) Human and rodent homologies in action control: corticostriatal determinants of goal-directed and habitual action. *Neuropsychopharmacology : official publication of the American College of Neuropsychopharmacology* 35:48-69.
- Bandelow B, Lichte T, Rudolf S, Wiltink J, Beutel ME (2015) The German guidelines for the treatment of anxiety disorders. *European archives of psychiatry and clinical neuroscience* 265:363-373.

## Bibliography

---

- Bandelow B et al. (2008) World Federation of Societies of Biological Psychiatry (WFSBP) guidelines for the pharmacological treatment of anxiety, obsessive-compulsive and post-traumatic stress disorders - first revision. *The world journal of biological psychiatry : the official journal of the World Federation of Societies of Biological Psychiatry* 9:248-312.
- Bandelow B et al. (2014) Deutsche S3-Leitlinie Behandlung von Angststörungen. Available at: [https://www.awmf.org/uploads/tx\\_szleitlinien/051-028l\\_S3\\_Angststoerungen\\_2014-05\\_1.pdf](https://www.awmf.org/uploads/tx_szleitlinien/051-028l_S3_Angststoerungen_2014-05_1.pdf) [Accessed March 12, 2019].
- Barkus C, McHugh SB, Sprengel R, Seeburg PH, Rawlins JN, Bannerman DM (2010) Hippocampal NMDA receptors and anxiety: at the interface between cognition and emotion. *European journal of pharmacology* 626:49-56.
- Bas-Hoogendam JM et al. (2017) Voxel-based morphometry multi-center mega-analysis of brain structure in social anxiety disorder. *NeuroImage Clinical* 16:678-688.
- Batalla A, Homberg JR, Lipina TV, Sescousse G, Luijten M, Ivanova SA, Schellekens AFA, Loonen AJM (2017) The role of the habenula in the transition from reward to misery in substance use and mood disorders. *Neuroscience and biobehavioral reviews* 80:276-285.
- Bedenk BT, Almeida-Correa S, Jurik A, Dedic N, Grunecker B, Genewsky AJ, Kaltwasser SF, Riebe CJ, Deussing JM, Czisch M, Wotjak CT (2018) Mn(2+) dynamics in manganese-enhanced MRI (MEMRI): Cav1.2 channel-mediated uptake and preferential accumulation in projection terminals. *NeuroImage* 169:374-382.
- Beique JC, Lin DT, Kang MG, Aizawa H, Takamiya K, Huganir RL (2006) Synapse-specific regulation of AMPA receptor function by PSD-95. *Proceedings of the National Academy of Sciences of the United States of America* 103:19535-19540.
- Belzung C, Le Pape G (1994) Comparison of different behavioral test situations used in psychopharmacology for measurement of anxiety. *Physiology & behavior* 56:623-628.
- Bennett MR (2011) The prefrontal-limbic network in depression: A core pathology of synapse regression. *Progress in neurobiology* 93:457-467.
- Benowitz LI, Routtenberg A (1997) GAP-43: an intrinsic determinant of neuronal development and plasticity. *Trends in neurosciences* 20:84-91.
- Biomarkers Definitions Working Group (2001) Biomarkers and surrogate endpoints: preferred definitions and conceptual framework. *Clinical pharmacology and therapeutics* 69:89-95.

- Bittner A, Goodwin RD, Wittchen HU, Beesdo K, Hofler M, Lieb R (2004) What characteristics of primary anxiety disorders predict subsequent major depressive disorder? *The Journal of clinical psychiatry* 65:618-626, quiz 730.
- Bora E, Harrison BJ, Davey CG, Yucel M, Pantelis C (2012) Meta-analysis of volumetric abnormalities in cortico-striatal-pallidal-thalamic circuits in major depressive disorder. *Psychological medicine* 42:671-681.
- Buresova O, Krekule I, Zahalka A, Bures J (1985) On-demand platform improves accuracy of the Morris water maze procedure. *Journal of neuroscience methods* 15:63-72.
- Calhoun GG, Tye KM (2015) Resolving the neural circuits of anxiety. *Nature neuroscience* 18:1394-1404.
- Carter RJ, Lione LA, Humby T, Mangiarini L, Mahal A, Bates GP, Dunnett SB, Morton AJ (1999) Characterization of progressive motor deficits in mice transgenic for the human Huntington's disease mutation. *The Journal of neuroscience : the official journal of the Society for Neuroscience* 19:3248-3257.
- Carter RM, Wittchen HU, Pfister H, Kessler RC (2001) One-year prevalence of subthreshold and threshold DSM-IV generalized anxiety disorder in a nationally representative sample. *Depression and anxiety* 13:78-88.
- Cesca F, Baldelli P, Valtorta F, Benfenati F (2010) The synapsins: key actors of synapse function and plasticity. *Progress in neurobiology* 91:313-348.
- Chen HJ, Rojas-Soto M, Oguni A, Kennedy MB (1998) A synaptic Ras-GTPase activating protein (p135 SynGAP) inhibited by CaM kinase II. *Neuron* 20:895-904.
- Chen X, Nelson CD, Li X, Winters CA, Azzam R, Sousa AA, Leapman RD, Gainer H, Sheng M, Reese TS (2011) PSD-95 is required to sustain the molecular organization of the postsynaptic density. *The Journal of neuroscience : the official journal of the Society for Neuroscience* 31:6329-6338.
- Choi SH, Kim YB, Paek SH, Cho ZH (2019) Papez Circuit Observed by in vivo Human Brain With 7.0T MRI Super-Resolution Track Density Imaging and Track Tracing. *Frontiers in neuroanatomy* 13:17.
- Conrad CD, Galea LA, Kuroda Y, McEwen BS (1996) Chronic stress impairs rat spatial memory on the Y maze, and this effect is blocked by tianeptine pretreatment. *Behavioral neuroscience* 110:1321-1334.

## Bibliography

---

- Conrad CD, LeDoux JE, Magarinos AM, McEwen BS (1999) Repeated restraint stress facilitates fear conditioning independently of causing hippocampal CA3 dendritic atrophy. *Behavioral neuroscience* 113:902-913.
- Costa RM, Cohen D, Nicoletis MA (2004) Differential corticostriatal plasticity during fast and slow motor skill learning in mice. *Current biology* : CB 14:1124-1134.
- Craske MG, Stein MB, Eley TC, Milad MR, Holmes A, Rapee RM, Wittchen HU (2017) Anxiety disorders. *Nature reviews Disease primers* 3:17024.
- Cryan JF, Holmes A (2005) Model organisms: The ascent of mouse: advances in modelling human depression and anxiety. *Nature Reviews Drug Discovery* 4:775-790.
- Cuijpers P, Dekker J, Hollon SD, Andersson G (2009) Adding psychotherapy to pharmacotherapy in the treatment of depressive disorders in adults: a meta-analysis. *The Journal of clinical psychiatry* 70:1219-1229.
- Dang MT, Yokoi F, Yin HH, Lovinger DM, Wang Y, Li Y (2006) Disrupted motor learning and long-term synaptic plasticity in mice lacking NMDAR1 in the striatum. *Proceedings of the National Academy of Sciences of the United States of America* 103:15254-15259.
- Davis M, Walker DL, Miles L, Grillon C (2010) Phasic vs sustained fear in rats and humans: role of the extended amygdala in fear vs anxiety. *Neuropsychopharmacology* : official publication of the American College of Neuropsychopharmacology 35:105-135.
- De Camilli P, Benfenati F, Valtorta F, Greengard P (1990) The synapsins. *Annual review of cell biology* 6:433-460.
- de Quervain DJ, Roozendaal B, McGaugh JL (1998) Stress and glucocorticoids impair retrieval of long-term spatial memory. *Nature* 394:787-790.
- DeFelipe J (2015) The dendritic spine story: an intriguing process of discovery. *Frontiers in neuroanatomy* 9:14.
- Diamond A (1990) Developmental time course in human infants and infant monkeys, and the neural bases of, inhibitory control in reaching. *Annals of the New York Academy of Sciences* 608:637-669; discussion 669-676.
- Diamond DM, Fleshner M, Ingersoll N, Rose GM (1996) Psychological stress impairs spatial working memory: relevance to electrophysiological studies of hippocampal function. *Behavioral neuroscience* 110:661-672.
- Dias GP, Bevilacqua MC, da Luz AC, Fleming RL, de Carvalho LA, Cocks G, Beckman D, Hosken LC, de Sant'Anna Machado W, Correa-e-Castro AC,

- Mousovich-Neto F, de Castro Gomes V, Bastos Gde N, Kubrusly RC, da Costa VM, Srivastava D, Landeira-Fernandez J, Nardi AE, Thuret S, Gardino PF (2014) Hippocampal biomarkers of fear memory in an animal model of generalized anxiety disorder. *Behavioural brain research* 263:34-45.
- Dias-Ferreira E, Sousa JC, Melo I, Morgado P, Mesquita AR, Cerqueira JJ, Costa RM, Sousa N (2009) Chronic stress causes frontostriatal reorganization and affects decision-making. *Science (New York, NY)* 325:621-625.
- Ehrlich I, Klein M, Rumpel S, Malinow R (2007) PSD-95 is required for activity-driven synapse stabilization. *Proceedings of the National Academy of Sciences of the United States of America* 104:4176-4181.
- Engert F, Bonhoeffer T (1999) Dendritic spine changes associated with hippocampal long-term synaptic plasticity. *Nature* 399:66-70.
- Fairen A, Peters A, Saldanha J (1977) A new procedure for examining Golgi impregnated neurons by light and electron microscopy. *Journal of neurocytology* 6:311-337.
- Femenia T, Gomez-Galan M, Lindskog M, Magara S (2012) Dysfunctional hippocampal activity affects emotion and cognition in mood disorders. *Brain research* 1476:58-70.
- Filiou MD, Asara JM, Nussbaumer M, Teplytska L, Landgraf R, Turck CW (2014) Behavioral extremes of trait anxiety in mice are characterized by distinct metabolic profiles. *Journal of psychiatric research* 58:115-122.
- Filiou MD, Zhang Y, Teplytska L, Reckow S, Gormanns P, Maccarrone G, Frank E, Kessler MS, Hamsch B, Nussbaumer M, Bunck M, Ludwig T, Yassouridis A, Holsboer F, Landgraf R, Turck CW (2011) Proteomics and metabolomics analysis of a trait anxiety mouse model reveals divergent mitochondrial pathways. *Biological psychiatry* 70:1074-1082.
- First MB, Bhat V, Adler D, Dixon L, Goldman B, Koh S, Levine B, Oslin D, Siris S (2014) How do clinicians actually use the Diagnostic and Statistical Manual of Mental Disorders in clinical practice and why we need to know more. *The Journal of nervous and mental disease* 202:841-844.
- Fletcher TL, Cameron P, De Camilli P, Banker G (1991) The distribution of synapsin I and synaptophysin in hippocampal neurons developing in culture. *The Journal of neuroscience : the official journal of the Society for Neuroscience* 11:1617-1626.
- Foy MR, Stanton ME, Levine S, Thompson RF (1987) Behavioral stress impairs long-term potentiation in rodent hippocampus. *Behavioral and neural biology* 48:138-149.

- Garthe A, Kempermann G (2013) An old test for new neurons: refining the Morris water maze to study the functional relevance of adult hippocampal neurogenesis. *Frontiers in neuroscience* 7:63.
- Genewsky A, Heinz DE, Kaplick PM, Kilonzo K, Wotjak CT (2017) A simplified microwave-based motion detector for home cage activity monitoring in mice. *Journal of biological engineering* 11:36.
- Genewsky A, Albrecht N, Bura SA, Kaplick PM, Heinz DE, Nußbaumer M, Engel M, Grünecker B, Kaltwasser SF, Riebe CJ, Bedenk BT, Czisch M, Wotjak CT (2018) How much fear is in anxiety? *bioRxiv:385823*.
- Gilad GM, Gilad VH, Wyatt RJ, Tizabi Y (1990) Region-selective stress-induced increase of glutamate uptake and release in rat forebrain. *Brain research* 525:335-338.
- Gipson CD, Olive MF (2017) Structural and functional plasticity of dendritic spines - root or result of behavior? *Genes, brain, and behavior* 16:101-117.
- Goslin K, Schreyer DJ, Skene JH, Banker G (1988) Development of neuronal polarity: GAP-43 distinguishes axonal from dendritic growth cones. *Nature* 336:672-674.
- Grahn JA, Parkinson JA, Owen AM (2009) The role of the basal ganglia in learning and memory: neuropsychological studies. *Behavioural brain research* 199:53-60.
- Grasselli G, Strata P (2013) Structural plasticity of climbing fibers and the growth-associated protein GAP-43. *Frontiers in neural circuits* 7:25.
- Gray EG (1959) Electron microscopy of synaptic contacts on dendrite spines of the cerebral cortex. *Nature* 183:1592-1593.
- Greengard P, Valtorta F, Czernik AJ, Benfenati F (1993) Synaptic vesicle phosphoproteins and regulation of synaptic function. *Science (New York, NY)* 259:780-785.
- Gregersen NO, Buttenschon HN, Hedemand A, Dahl HA, Kristensen AS, Clementsen B, Woldbye DP, Koefoed P, Erhardt A, Kruse TA, Wang AG, Borglum AD, Mors O (2014) Are TMEM genes potential candidate genes for panic disorder? *Psychiatric genetics* 24:37-41.
- Gross CT, Canteras NS (2012) The many paths to fear. *Nature reviews Neuroscience* 13:651-658.

## Bibliography

---

- Hamidi A (2015) The Rotarod Test (For Mice). Available at: <https://mazeengineers.com/maze-basics-rotarod-test-for-mice/> [Accessed February 11, 2019].
- Hering H, Sheng M (2001) Dendritic spines: structure, dynamics and regulation. *Nature reviews Neuroscience* 2:880-888.
- Hettema JM, Kettenmann B, Ahluwalia V, McCarthy C, Kates WR, Schmitt JE, Silberg JL, Neale MC, Kendler KS, Fatouros P (2012) Pilot multimodal twin imaging study of generalized anxiety disorder. *Depression and anxiety* 29:202-209.
- Hilbert K, Lueken U, Beesdo-Baum K (2014) Neural structures, functioning and connectivity in Generalized Anxiety Disorder and interaction with neuroendocrine systems: a systematic review. *Journal of affective disorders* 158:114-126.
- Hilbert K, Pine DS, Muehlhan M, Lueken U, Steudte-Schmiedgen S, Beesdo-Baum K (2015) Gray and white matter volume abnormalities in generalized anxiety disorder by categorical and dimensional characterization. *Psychiatry research* 234:314-320.
- Holahan MR (2017) A Shift from a Pivotal to Supporting Role for the Growth-Associated Protein (GAP-43) in the Coordination of Axonal Structural and Functional Plasticity. *Frontiers in cellular neuroscience* 11:266.
- Holsboer F, Ströhle A (2005) *Anxiety and Anxiolytic Drugs*. Berlin, Heidelberg, New York: Springer. p: 37
- Horner AE, Heath CJ, Hvoslef-Eide M, Kent BA, Kim CH, Nilsson SR, Alsio J, Oomen CA, Holmes A, Saksida LM, Bussey TJ (2013) The touchscreen operant platform for testing learning and memory in rats and mice. *Nature protocols* 8:1961-1984.
- Jurado-Arjona J, Rodriguez-Matellan A, Avila J, Hernandez F (2019) GSK3beta overexpression driven by GFAP promoter improves rotarod performance. *Brain research* 1712:47-54.
- Juszczak GR, Miller M (2016) Detour Behavior of Mice Trained with Transparent, Semitransparent and Opaque Barriers. *PloS one* 11:e0162018.
- Kabadayi C, Bobrowicz K, Osvath M (2018) The detour paradigm in animal cognition. *Animal cognition* 21:21-35.
- Kassem MS, Lagopoulos J, Stait-Gardner T, Price WS, Chohan TW, Arnold JC, Hatton SN, Bennett MR (2013) Stress-induced grey matter loss determined by

- MRI is primarily due to loss of dendrites and their synapses. *Molecular neurobiology* 47:645-661.
- Kawasaki A, Okada M, Tamada A, Okuda S, Nozumi M, Ito Y, Kobayashi D, Yamasaki T, Yokoyama R, Shibata T, Nishina H, Yoshida Y, Fujii Y, Takeuchi K, Igarashi M (2018) Growth Cone Phosphoproteomics Reveals that GAP-43 Phosphorylated by JNK Is a Marker of Axon Growth and Regeneration. *iScience* 4:190-203.
- Kempton MJ, Salvador Z, Munafo MR, Geddes JR, Simmons A, Frangou S, Williams SC (2011) Structural neuroimaging studies in major depressive disorder. Meta-analysis and comparison with bipolar disorder. *Archives of general psychiatry* 68:675-690.
- Kesner RP (2013) A process analysis of the CA3 subregion of the hippocampus. *Frontiers in cellular neuroscience* 7:78.
- Kesner RP, Rolls ET (2015) A computational theory of hippocampal function, and tests of the theory: new developments. *Neuroscience and biobehavioral reviews* 48:92-147.
- Kim E, Sheng M (2004) PDZ domain proteins of synapses. *Nature reviews Neuroscience* 5:771-781.
- Kim JH, Liao D, Lau LF, Huganir RL (1998) SynGAP: a synaptic RasGAP that associates with the PSD-95/SAP90 protein family. *Neuron* 20:683-691.
- Kim JJ, Foy MR, Thompson RF (1996) Behavioral stress modifies hippocampal plasticity through N-methyl-D-aspartate receptor activation. *Proceedings of the National Academy of Sciences of the United States of America* 93:4750-4753.
- Krapivinsky G, Medina I, Krapivinsky L, Gapon S, Clapham DE (2004) SynGAP-MUPP1-CaMKII synaptic complexes regulate p38 MAP kinase activity and NMDA receptor-dependent synaptic AMPA receptor potentiation. *Neuron* 43:563-574.
- Krömer SA, Kessler MS, Milfay D, Birg IN, Bunck M, Czibere L, Panhuysen M, Putz B, Deussing JM, Holsboer F, Landgraf R, Turck CW (2005) Identification of glyoxalase-I as a protein marker in a mouse model of extremes in trait anxiety. *The Journal of neuroscience : the official journal of the Society for Neuroscience* 25:4375-4384.
- Lago T, Davis A, Grillon C, Ernst M (2017) Striatum on the anxiety map: Small detours into adolescence. *Brain research* 1654:177-184.

## Bibliography

---

- Landgraf R, Wigger A (2003) Born to be anxious: neuroendocrine and genetic correlates of trait anxiety in HAB rats. *Stress (Amsterdam, Netherlands)* 6:111-119.
- Landgraf R, Kessler MS, Bunck M, Murgatroyd C, Spengler D, Zimbelmann M, Nussbaumer M, Czibere L, Turck CW, Singewald N, Rujescu D, Frank E (2007) Candidate genes of anxiety-related behavior in HAB/LAB rats and mice: focus on vasopressin and glyoxalase-I. *Neuroscience and biobehavioral reviews* 31:89-102.
- Latchney SE, Masiulis I, Zaccaria KJ, Lagace DC, Powell CM, McCasland JS, Eisch AJ (2014) Developmental and adult GAP-43 deficiency in mice dynamically alters hippocampal neurogenesis and mossy fiber volume. *Developmental neuroscience* 36:44-63.
- LeDoux JE, Pine DS (2016) Using Neuroscience to Help Understand Fear and Anxiety: A Two-System Framework. *The American journal of psychiatry* 173:1083-1093.
- Lee KF, Soares C, Beique JC (2012) Examining form and function of dendritic spines. *Neural plasticity* 2012:704103.
- Lee T, Jarome T, Li SJ, Kim JJ, Helmstetter FJ (2009) Chronic stress selectively reduces hippocampal volume in rats: a longitudinal magnetic resonance imaging study. *Neuroreport* 20:1554-1558.
- Liao M, Yang F, Zhang Y, He Z, Song M, Jiang T, Li Z, Lu S, Wu W, Su L, Li L (2013) Childhood maltreatment is associated with larger left thalamic gray matter volume in adolescents with generalized anxiety disorder. *PLoS one* 8:e71898.
- Lister RG (1987) The use of a plus-maze to measure anxiety in the mouse. *Psychopharmacology* 92:180-185.
- Lopez-Munoz F, Boya J, Alamo C (2006) Neuron theory, the cornerstone of neuroscience, on the centenary of the Nobel Prize award to Santiago Ramon y Cajal. *Brain research bulletin* 70:391-405.
- Luine V, Villegas M, Martinez C, McEwen BS (1994) Repeated stress causes reversible impairments of spatial memory performance. *Brain research* 639:167-170.
- Maguire EA, Burgess N, Donnett JG, Frackowiak RS, Frith CD, O'Keefe J (1998) Knowing where and getting there: a human navigation network. *Science (New York, NY)* 280:921-924.

- Marchand WR (2010) Cortico-basal ganglia circuitry: a review of key research and implications for functional connectivity studies of mood and anxiety disorders. *Brain structure & function* 215:73-96.
- Martin SJ, Grimwood PD, Morris RG (2000) Synaptic plasticity and memory: an evaluation of the hypothesis. *Annual review of neuroscience* 23:649-711.
- Matsuzaki M, Honkura N, Ellis-Davies GC, Kasai H (2004) Structural basis of long-term potentiation in single dendritic spines. *Nature* 429:761-766.
- Mazzarello P (2018) From images to physiology: A strange paradox at the origin of modern neuroscience. *Progress in brain research* 243:233-256.
- McKinney WT, Jr., Bunney WE, Jr. (1969) Animal model of depression. I. Review of evidence: implications for research. *Archives of general psychiatry* 21:240-248.
- McNaughton N, Gray JA (2000) Anxiolytic action on the behavioural inhibition system implies multiple types of arousal contribute to anxiety. *Journal of affective disorders* 61:161-176.
- Meyer D, Bonhoeffer T, Scheuss V (2014) Balance and stability of synaptic structures during synaptic plasticity. *Neuron* 82:430-443.
- Moon CM, Jeong GW (2017) Abnormalities in gray and white matter volumes associated with explicit memory dysfunction in patients with generalized anxiety disorder. *Acta radiologica (Stockholm, Sweden : 1987)* 58:353-361.
- Moon CM, Kim GW, Jeong GW (2014) Whole-brain gray matter volume abnormalities in patients with generalized anxiety disorder: voxel-based morphometry. *Neuroreport* 25:184-189.
- Morita S, Miyata S (2013) Synaptic localization of growth-associated protein 43 in cultured hippocampal neurons during synaptogenesis. *Cell biochemistry and function* 31:400-411.
- Morris R (1984) Developments of a water-maze procedure for studying spatial learning in the rat. *Journal of neuroscience methods* 11:47-60.
- Morris RG (2003) Long-term potentiation and memory. *Philosophical transactions of the Royal Society of London Series B, Biological sciences* 358:643-647.
- Murakoshi H, Yasuda R (2012) Postsynaptic signaling during plasticity of dendritic spines. *Trends in neurosciences* 35:135-143.

## Bibliography

---

- Nikolaev M, Heggelund P (2015) Functions of synapsins in corticothalamic facilitation: important roles of synapsin I. *The Journal of physiology* 593:4499-4510.
- O'Keefe J, Nadel L (1978) *The hippocampus as a cognitive map*. Oxford: Oxford University Press.
- O'Keefe J, Burgess N, Donnett JG, Jeffery KJ, Maguire EA (1998) Place cells, navigational accuracy, and the human hippocampus. *Philosophical transactions of the Royal Society of London Series B, Biological sciences* 353:1333-1340.
- Ormel J et al. (2008) Disability and treatment of specific mental and physical disorders across the world. *The British journal of psychiatry : the journal of mental science* 192:368-375.
- Papez JW (1995) A proposed mechanism of emotion. 1937. *The Journal of neuropsychiatry and clinical neurosciences* 7:103-112.
- Parfitt GM, Nguyen R, Bang JY, Aqrabawi AJ, Tran MM, Seo DK, Richards BA, Kim JC (2017) Bidirectional Control of Anxiety-Related Behaviors in Mice: Role of Inputs Arising from the Ventral Hippocampus to the Lateral Septum and Medial Prefrontal Cortex. *Neuropsychopharmacology : official publication of the American College of Neuropsychopharmacology* 42:1715-1728.
- Pellow S, Chopin P, File SE, Briley M (1985) Validation of open:closed arm entries in an elevated plus-maze as a measure of anxiety in the rat. *Journal of neuroscience methods* 14:149-167.
- Pollerberg GE, Thelen K, Theiss MO, Hochlehnert BC (2013) The role of cell adhesion molecules for navigating axons: density matters. *Mechanisms of development* 130:359-372.
- Porter JN, Roy AK, Benson B, Carlisi C, Collins PF, Leibenluft E, Pine DS, Luciana M, Ernst M (2015) Age-related changes in the intrinsic functional connectivity of the human ventral vs. dorsal striatum from childhood to middle age. *Developmental cognitive neuroscience* 11:83-95.
- Ramirez-Amaya V, Escobar ML, Chao V, Bermudez-Rattoni F (1999) Synaptogenesis of mossy fibers induced by spatial water maze overtraining. *Hippocampus* 9:631-636.
- Ramirez-Amaya V, Balderas I, Sandoval J, Escobar ML, Bermudez-Rattoni F (2001) Spatial long-term memory is related to mossy fiber synaptogenesis. *The Journal of neuroscience : the official journal of the Society for Neuroscience* 21:7340-7348.

- Rebola N, Carta M, Mulle C (2017) Operation and plasticity of hippocampal CA3 circuits: implications for memory encoding. *Nature reviews Neuroscience* 18:208-220.
- Rice DP, Miller LS (1998) Health economics and cost implications of anxiety and other mental disorders in the United States. *The British journal of psychiatry Supplement*:4-9.
- Rolls ET (2007) An attractor network in the hippocampus: theory and neurophysiology. *Learning & memory (Cold Spring Harbor, NY)* 14:714-731.
- Ruediger S, Vittori C, Bednarek E, Genoud C, Strata P, Sacchetti B, Caroni P (2011) Learning-related feedforward inhibitory connectivity growth required for memory precision. *Nature* 473:514-518.
- Salunke BP, Umathe SN, Chavan JG (2014) Involvement of NMDA receptor in low-frequency magnetic field-induced anxiety in mice. *Electromagnetic biology and medicine* 33:312-326.
- Scholz J, Niibori Y, P WF, J PL (2015) Rotarod training in mice is associated with changes in brain structure observable with multimodal MRI. *NeuroImage* 107:182-189.
- Siegmund A, Wotjak CT (2006) Toward an animal model of posttraumatic stress disorder. *Annals of the New York Academy of Sciences* 1071:324-334.
- Soria-Gomez E, Busquets-Garcia A, Hu F, Mehidi A, Cannich A, Roux L, Louit I, Alonso L, Wiesner T, Georges F, Verrier D, Vincent P, Ferreira G, Luo M, Marsicano G (2015) Habenular CB1 Receptors Control the Expression of Aversive Memories. *Neuron* 88:306-313.
- Sousa N, Lukoyanov NV, Madeira MD, Almeida OF, Paula-Barbosa MM (2000) Reorganization of the morphology of hippocampal neurites and synapses after stress-induced damage correlates with behavioral improvement. *Neuroscience* 97:253-266.
- Spiers HJ, Gilbert SJ (2015) Solving the detour problem in navigation: a model of prefrontal and hippocampal interactions. *Frontiers in human neuroscience* 9:125.
- Spooner RI, Thomson A, Hall J, Morris RG, Salter SH (1994) The Atlantis platform: a new design and further developments of Buresova's on-demand platform for the water maze. *Learning & memory (Cold Spring Harbor, NY)* 1:203-211.
- Stepan J, Dine J, Fenzl T, Polta SA, von Wolff G, Wotjak CT, Eder M (2012) Entorhinal theta-frequency input to the dentate gyrus trisynaptically evokes hippocampal CA1 LTP. *Frontiers in neural circuits* 6:64.

## Bibliography

---

- Su Q, Zhang H, Dang S, Yao D, Shao S, Zhu Z, Li H (2019) Hippocampal Protein Kinase C Gamma Signaling Mediates the Impairment of Spatial Learning and Memory in Prenatally Stressed Offspring Rats. *Neuroscience* 414:186-199.
- Sunanda, Rao MS, Raju TR (1995) Effect of chronic restraint stress on dendritic spines and excrescences of hippocampal CA3 pyramidal neurons--a quantitative study. *Brain research* 694:312-317.
- Tasan RO, Bukovac A, Peterschmitt YN, Sartori SB, Landgraf R, Singewald N, Sperk G (2011) Altered GABA transmission in a mouse model of increased trait anxiety. *Neuroscience* 183:71-80.
- Treves A, Rolls ET (1994) Computational analysis of the role of the hippocampus in memory. *Hippocampus* 4:374-391.
- Tucci V, Achilli F, Blanco G, Lad HV, Wells S, Godinho S, Nolan PM (2007) Reaching and grasping phenotypes in the mouse (*Mus musculus*): a characterization of inbred strains and mutant lines. *Neuroscience* 147:573-582.
- Vorhees CV, Williams MT (2006) Morris water maze: procedures for assessing spatial and related forms of learning and memory. *Nature protocols* 1:848-858.
- Vyas A, Mitra R, Shankaranarayana Rao BS, Chattarji S (2002) Chronic stress induces contrasting patterns of dendritic remodeling in hippocampal and amygdaloid neurons. *The Journal of neuroscience : the official journal of the Society for Neuroscience* 22:6810-6818.
- Wang L, Lu H, Brown PL, Rea W, Vaupel B, Yang Y, Stein E, Shepard PD (2015) Manganese-Enhanced MRI Reflects Both Activity-Independent and Activity-Dependent Uptake within the Rat Habenulomesencephalic Pathway. *PloS one* 10:e0127773.
- Wang SH, Morris RG (2010) Hippocampal-neocortical interactions in memory formation, consolidation, and reconsolidation. *Annual review of psychology* 61:49-79, c41-44.
- Watanabe Y, Gould E, McEwen BS (1992) Stress induces atrophy of apical dendrites of hippocampal CA3 pyramidal neurons. *Brain research* 588:341-345.
- Wigger A, Sanchez MM, Mathys KC, Ebner K, Frank E, Liu D, Kresse A, Neumann ID, Holsboer F, Plotsky PM, Landgraf R (2004) Alterations in central neuropeptide expression, release, and receptor binding in rats bred for high anxiety: critical role of vasopressin. *Neuropsychopharmacology : official publication of the American College of Neuropsychopharmacology* 29:1-14.

## Bibliography

---

- Wittchen HU (2002) Generalized anxiety disorder: prevalence, burden, and cost to society. *Depression and anxiety* 16:162-171.
- Wittchen HU, Kessler RC, Pfister H, Lieb M (2000) Why do people with anxiety disorders become depressed? A prospective-longitudinal community study. *Acta psychiatrica Scandinavica Supplementum*:14-23.
- Wittchen HU, Jacobi F, Rehm J, Gustavsson A, Svensson M, Jonsson B, Olesen J, Allgulander C, Alonso J, Faravelli C, Fratiglioni L, Jennum P, Lieb R, Maercker A, van Os J, Preisig M, Salvador-Carulla L, Simon R, Steinhausen HC (2011) The size and burden of mental disorders and other disorders of the brain in Europe 2010. *European neuropsychopharmacology : the journal of the European College of Neuropsychopharmacology* 21:655-679.
- Yamaguchi T, Danjo T, Pastan I, Hikida T, Nakanishi S (2013) Distinct roles of segregated transmission of the septo-habenular pathway in anxiety and fear. *Neuron* 78:537-544.
- Yang Y, Tao-Cheng JH, Bayer KU, Reese TS, Dosemeci A (2013) Camkii-mediated phosphorylation regulates distributions of Syngap-alpha1 and -alpha2 at the postsynaptic density. *PloS one* 8:e71795.
- Yen YC, Mauch CP, Dahlhoff M, Micale V, Bunck M, Sartori SB, Singewald N, Landgraf R, Wotjak CT (2012) Increased levels of conditioned fear and avoidance behavior coincide with changes in phosphorylation of the protein kinase B (AKT) within the amygdala in a mouse model of extremes in trait anxiety. *Neurobiology of learning and memory* 98:56-65.
- Yin HH, Knowlton BJ, Balleine BW (2006) Inactivation of dorsolateral striatum enhances sensitivity to changes in the action-outcome contingency in instrumental conditioning. *Behavioural brain research* 166:189-196.
- Yin HH, Ostlund SB, Knowlton BJ, Balleine BW (2005) The role of the dorsomedial striatum in instrumental conditioning. *The European journal of neuroscience* 22:513-523.
- Yin HH, Mulcare SP, Hilario MR, Clouse E, Holloway T, Davis MI, Hansson AC, Lovinger DM, Costa RM (2009) Dynamic reorganization of striatal circuits during the acquisition and consolidation of a skill. *Nature neuroscience* 12:333-341.

## Acknowledgment

I would like to thank all the people without whose efforts and support my project would not have been possible. First of all, I want to thank PD Dr. Angelika Erhardt who thankfully took over the official supervision of my doctoral thesis at the Ludwig Maximilian University Munich.

I would like to emphasize my gratitude to PD Dr. Carsten T. Wotjak who supervised and supported me with all his remarkable knowledge and expertise. He gave me the possibility to gain valuable insights into basic research. All this, together with his optimistic attitude and sayings suiting any situation made this time an enriching experience.

Especially I would like to thank my direct supervisor Daniel E. Heinz for his supportive, open, professional and human way throughout my entire time at the Max Planck Institute. I really appreciate his exceptional commitment and ambition to accomplish the best possible outcome. In combination with all his knowledge, patience and encouraging words he has been the best possible direct supervisor.

For the support in the neuroimaging part, I also want to thank Dr. Michael Czisch who taught me how to operate the MRI and explained to me the physical backgrounds in a comprehensible way. For their support in how to handle the NeuroLucida software, I want to thank Dr. Matthias Eder and, especially Srivaishnavi Loganathan who additionally helped me with the Golgi staining and the unbiased neuron selection. Furthermore, I would like to thank Mojan Parvaz for her assistance in performing the western blot and the good conversations we had.

Last but not least I would like to thank my wonderful extended family and friends for their support and belief in me. I am really grateful to have each and every one of you around me. Especially I want to thank Peter Gerlach for his sustained unconditional support.

## Affidivat

### Eidesstattliche Versicherung

Bartmann, Marie Karolin Franziska

---

Name, Vorname

Ich erkläre hiermit an Eides statt,  
dass ich die vorliegende Dissertation mit dem Titel

Anatomy, structure and function: Understanding extremes in fear and anxiety by in vivo imaging techniques

selbständig verfasst, mich außer der angegebenen keiner weiteren Hilfsmittel bedient und alle Erkenntnisse, die aus dem Schrifttum ganz oder annähernd übernommen sind, als solche kenntlich gemacht und nach ihrer Herkunft unter Bezeichnung der Fundstelle einzeln nachgewiesen habe.

Ich erkläre des Weiteren, dass die hier vorgelegte Dissertation nicht in gleicher oder in ähnlicher Form bei einer anderen Stelle zur Erlangung eines akademischen Grades eingereicht wurde.

Bad Tölz, 25.03.2022

Marie Bartmann

Ort, Datum

Unterschrift Doktorandin bzw. Doktorand